ADVANCED ENERGY MATERIALS
www.advenergymat.de

Progress and Perspectives of Organosulfur for Lithium–Sulfur Batteries

Zhiyong Pan, Dan J. L. Brett, Guanjie He, and Ivan P. Parkin**

Lithium–sulfur batteries (LSBs) with high theoretical capacity are regarded as the most promising candidates for next-generation energy storage systems. However, the low conductivity, high volume change, and shuttle effect need to be addressed before the commercialization of LSBs. Organosulfur with covalent C—S bonds can solve these problems when applied as different components of LSBs. Recent advances of application of organosulfur as cathodes, electrolytes, interlayers, and binders in LSBs are reviewed. Finally, the prospects for organosulfur are proposed from both the perspectives of mechanism understanding and practical applications.

1. Introduction

The ever-increasing application of electronic devices, including mobile phones and electric vehicles, in daily life and the concerns about environmental issues have expedited the development of a new energy storage industry.[1–3] So far, lithium-ion batteries (LIBs) using layered lithium transition metal oxide as the cathode and graphite as the anode have been the most successful and widely used energy storage technology.[4–6] While the energy density of LIBs has been promoted to about 300 W h kg^{-1} over the past decades, further development is hindered by the theoretical capacity of the layered lithium transition metal oxide cathode.[7–9] Thus, developing new electrode materials and energy storage technology is necessary.

Z. Pan, G. He, I. P. Parkin
Christopher Ingold Laboratory
Department of Chemistry
University College London
20 Gordon Street, London WC1H 0AJ, UK
E-mail: g.he@ucl.ac.uk; i.p.parkin@ucl.ac.uk
D. J. L. Brett, G. He
Electrochemical Innovation Lab
Department Chemical Engineering
University College London
London WC1E 7JE, UK
G. He
School of Chemistry
University of Lincoln
Joseph Banks Laboratories
Green Lane, Lincoln LN6 7DL, UK
The ORCID identification number(s) for the author(s) of this article can be found under https://doi.org/10.1002/aenm.202103483.

DOI: 10.1002/aenm.202103483

Lithium–sulfur batteries (LSBs) are one of the most promising candidates for post-LIBs technologies.[10–12] In LSBs, a theoretical capacity of 1675 mA h g^{-1} can be achieved through a multi-electron reaction between sulfur and lithium. Two distinguishing voltage plateaus occur during the discharge process. At the higher voltage plateau (about 2.3 V), the ring structure of S_8, the most stable allotrope of S, is destroyed, and long chain lithium polysulfides are formed; Li_2S_8 at the beginning and then further reduced to Li_2S_6 and Li_2S_4. At the lower voltage plateau (about 2.1 V), long chain lithium polysulfides are further reduced to Li_2S_2 and Li_2S.[13,14] Besides the high theoretical capacity, the abundance of S on Earth, low price and environment-friendly properties make LSBs conceivably cheaper than LIBs. However, several obstacles stand in the way of the industrialization of LSBs.[15,16] First, S as well as the discharge product Li_2S is intrinsically insulating ($\approx 5 \times 10^{-30}$ S cm^{-1}). The low electrical conductivity of electrode materials will affect electrochemical properties of batteries especially at high current densities. Second, big volume change during charge and discharge results in safety and stability issues. Due to the differences in density of S and Li_2S, a volume change as high as 75% will take place when S is transferred to Li_2S. Finally, the notorious shuttle effect further causes performance decay. Lithium polysulfides formed during charge and discharge are soluble in electrolytes. These intermediates shuttle between cathodes and anodes and react with electrode materials through chemical or electrochemical reactions as shown in Equations (1) and (2), leading to the consumption of the lithium anode and the formation of "dead" sulfur and finally low Coulombic efficiency and stability.

$$2Li_2S_6 + 2Li = 3Li_2S_4 \quad (1)$$

$$Li_2S_4 + 2S = Li_2S_6 \quad (2)$$

Several strategies have been proposed by researchers to solve these problems, mainly focused on the shuttle effect, over the past decades. First, carbon materials with porous structures have been used as hosts for S.[17,18] The porous structure provides a space constrain and makes the diffusion of lithium polysulfides more difficult. In these structures, the carbon framework provides good electrical conductivity while the porous structure accommodates the volume change and also confines lithium polysulfides to the pores and alleviates the shuttle effect. However, due to the non-polarity of carbon materials, physical confinement of lithium polysulfides is insufficient. Instead, transition metal oxides and sulfides with strong chemical adsorption of lithium polysulfides have been widely studied in LSBs.[19,20] On the surface of these

materials, strong intercalations will form between transition metal oxides/sulfides with lithium polysulfides through van der Waals interaction force or Lewis acid and base intercalation. The polysulfide anions with extra lone pair electrons act as Lewis bases while the transition metal oxides/sulfides act as Lewis acids. Although physical confinement and chemical adsorption can alleviate the shuttle effect, the blocked polysulfides cannot be fully used especially at high sulfur loading, under which condition the concentration of lithium polysulfides could be so high that it exceeds the confinement or adsorption limitation. Thus, compounds with catalytic activities to promote the sluggish reactions have been widely studied in LSBs.[21,22] So far, these catalysts are mainly transition metal oxides/sulfides/nitrides or metal atoms. Besides these strategies, recently, organosulfur has been widely studied because of its inherent merits.[23–25] The fabrication of organosulfur compounds is often easier compared with the synthesis of transition metal-based compounds. Organosulfur compounds are inexpensive and environmentally friendly. More importantly, the organosulfur provides a structure to suppress shuttle effects. Sulfur is embedded in the framework and covalently bonded with carbon or other heteroatoms. Though there have been lots of reviews about LSBs, for example Manthiram et al. published a comprehensive review about each component of LSBs,[3] and Lim et al. published a review focused on catalytic materials in LSBs,[26] previous reviews with the focus on the application of organosulfur in LSBs are rare.

In this review, the recent progress of organosulfur compounds in LSBs is provided. The organosulfur compounds are classified into three types: small organosulfur molecules, high sulfur content copolymers, and sulfurized polymers. The application of organosulfur compounds in cathode materials, electrolytes, interlayers (a functional layer between cathode and separator) as well as binders are all reviewed. Finally, the research status, both advances and challenges, of organosulfur in LSBs are summarized and an outlook is provided.

2. Organosulfur as Cathode Materials for Lithium–Sulfur Batteries

Cathode materials are crucial for LSBs. The energy density of LSBs mainly depends on the capacity of sulfur cathodes, when lithium metal anode is used. The efficiency and cyclic stability of LSBs mainly depend on whether the sulfur cathodes can successfully suppress the shuttle effect. Consequently, there are thousands of research articles about designing and synthesizing cathode materials for high-performance LSBs over the past decades. By optimizing the structures and components of cathode materials, the shuttle effect can be alleviated through the different strategies mentioned above. However, these cathode materials often have a complicated and expensive fabrication process. Meanwhile, organosulfur compounds are easy to synthesize, but special attention needs to be paid during the synthesis process as toxic gases as SO_2 and H_2S may be released, side reactions may take place, and are environmentally friendly, thus drawing more and more recent attention. Organosulfur compounds can be classified into three types based on their structures, synthesis methods, and electrochemical performances: small organosulfur molecules, high sulfur content copolymers, and sulfurized polymers (**Figure 1**). Small organosulfur molecules are organic molecules that have several sulfur atoms. Because of the short sulfur chain, usually less than four sulfur atoms in one molecule, the formation of lithium polysulfides during charge and discharge processes vanishes. This type of organic molecules is usually soluble in the organic electrolyte used in LSBs, which is suitable for use as an electrolyte additive. However, when used as the electrode material, a host is needed to prevent it from dissolving into the electrolytes and reacting with the Li anodes directly. High sulfur content copolymers are fabricated through the copolymerization of sulfur and unsaturated organic monomers. A cross-linked structure is formed as sulfur is grafted to the main chain of the polymer. The physical and chemical properties of these compounds can be modulated by designing monomers with different structures and controlling the ratio of sulfur and monomer during the copolymerization. Sulfurized polymers are synthesized through a high temperature treatment of a mixture of sulfur and polymers. Polymers with unsaturated groups in their main chain or side chain will react with sulfur to form ring structures or cross-linked structures. All three types of organosulfur materials can be used as cathode materials for LSBs. However, the differences in structures between these compounds result in different physical and electrochemical performances.

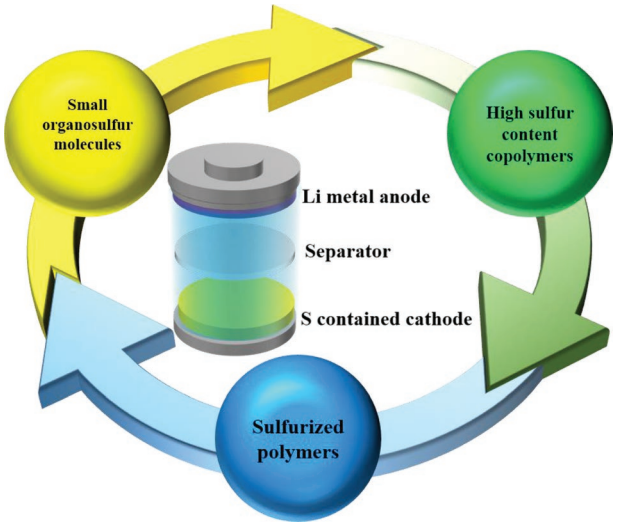

Figure 1. Schematic diagram of organosulfur in lithium-sulfur batteries (LSBs).

3. Small Organosulfur Molecules

In 1988, Visco et al. first reported a battery system that worked through the chemically reversible oxidation of alkali metal thiol salts to corresponding disulfides ($2\ RS^- \rightleftharpoons RSSR + 2\ e^-$).[27] Since then, small organosulfur molecules have been widely studied in different energy storage systems, including LSBs.

Manthiram's group studied the application of a variety of small organosulfur molecules as electrode materials for batteries. In 2020, they reported the application of Xanthogen polysulfides as the cathode material for the first time. Xanthogen polysulfides have a formula of R–O–C(S)–S–S_n–S–(S)C–O–R,

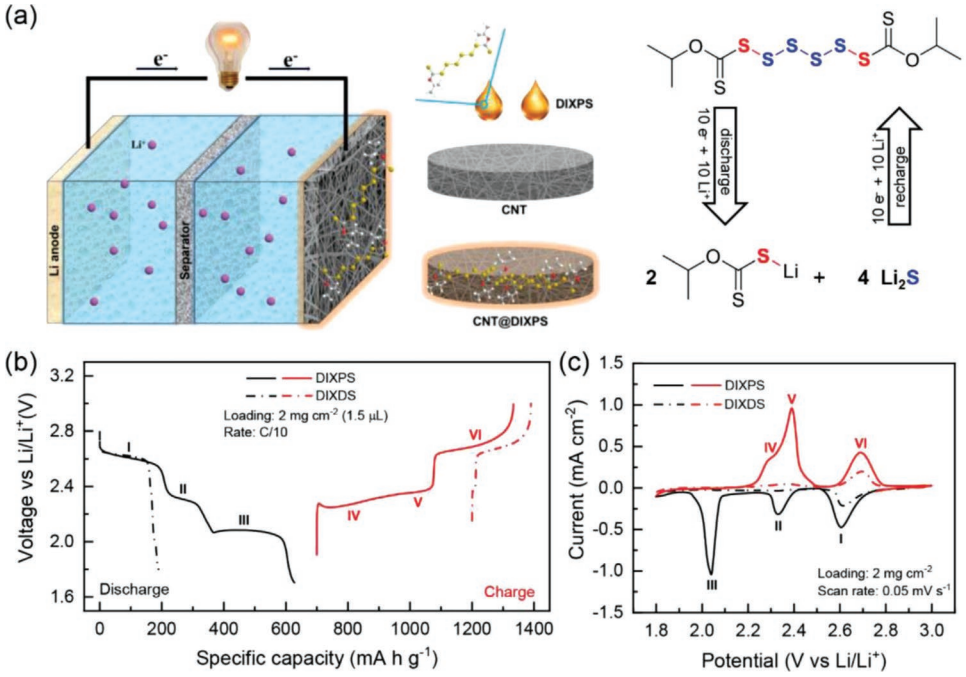

Figure 2. a) Schematic of the cell configuration. b) Voltage profiles for di-isopropyl xanthogen polysulfide (DIXPS) and di-isopropyl xanthogen disulfide (DIXDS) when cycled at 0.1 C (1 C = 672 mA g^{-1} for DIXPS; 1 C = 198 mA g^{-1} for DIXDS). c) Cyclic voltammograms (CV) of the first cycle for DIXPS and DIXDS at a scan rate of 0.05 mV s^{-1}. Reproduced with permission.[28] Copyright 2020, Wiley-VCH.

where R is an alkyl or aryl group, *n* is the number of sulfur atoms and C(S) is a double bond between C and S (**Figure 2**a).[28] The materials with different numbers of sulfur atoms were synthesized and characterized: di-isopropyl xanthogen disulfide (DIXDS) and di-isopropyl xanthogen polysulfide (DIXPS). The number of sulfur atoms affects both physical and electrochemical properties of these compounds. DIXDS with only two sulfur atoms is a light-yellow solid powder, while DIXPS is a yellow liquid; free-standing carbon nanotube (CNT) paper was used to confine the liquid in the batteries. DIXDS showed only one voltage plateau, DIXPS showed three voltage plateaus: 2.61, 2.30, and 2.08 V (Figure 2b,c). The voltage plateaus at 2.30 and 2.08 V were ascribed to the conversion of linear sulfur to Li_2S, while the highest voltage plateau originated from the disulfide-thiolate redox occurring at the terminal xanthogen groups. The inductive and mesomeric effects of xanthogen groups lead to electron-withdrawal from terminal sulfur atoms, and thus the electrochemical potential is higher than other sulfur atoms; apparently more sulfur atoms means higher specific capacity. An initial capacity of 628 mA h g^{-1} at 0.1 C (1 C = 672 mA g^{-1}) was delivered by DIXPS, about two times higher than that of DIXDS. Meanwhile, a prolonged cycling (1000 cycles) stability at a high rate of 4 C with a low capacity decay rate of 0.026% was achieved.

He et al. employed dimethyl trisulfide (DMTS, CH_3SSSCH_3) as a model compound to investigate the capacity fading mechanism of organosulfur materials and proposed a solution.[29] As DMTS is soluble in the electrolyte, 3D graphene sponge and those with nitrogen doping and Fe_3O_4 decorating (3DG, 3DNG and 3DFNG) were used as the host for DMTS. It was found that materials with 3DFNG as the host showed the best electrochemical performance: high initial capacity (822 mA h g^{-1} at 0.1 C), better rate performance, and superior long cycle stability (500 cycles with a capacity decay rate of 0.09% per cycle). The visual test showed that the cell with 3DFNG had no obvious color change while those with 3DG and 3DNG turned yellow and brown after working for certain time. This phenomenon suggested that DMTS and the discharge products (CH_3–S–Li and CH_3–S–S–Li) were soluble in the electrolyte exhibiting similar solubility as lithium polysulfides. As a result, these compounds would diffuse to the anode and passivate lithium metals. Because 3DFNG had the highest adsorption ability of intermediates and prevented side reactions, the batteries with 3DFNG hosts had the best performance. The ^1H nuclear magnetic resonance (NMR) also revealed a weaker peak intensity of CH_3–S–Li in the cell with 3DFNG host.

Thiols are another type of organic compounds that easily react with sulfur to form products with long sulfur chains (2 RSH + n S = R–S–S_{n-1}–S–R + H_2S). Bhargav et al. reported a facial and scalable route to synthesize phenyl polysulfides: phenyl tetrasulfide, phenyl pentasulfide, and phenyl hexasulfide (PHS), as shown in **Figure 3**.[30] The relationship between the length of the sulfur chain in phenyl polysulfides and the volume change of electrodes was revealed. In C/S composite electrodes, the volume change can reach 80%, which will lead to the fracture of electrodes and the poor stability. However, when utilizing phenyl polysulfides, the volume change can be reduced to 37%, less than half of that in C/S composites. Phenyl polysulfides had three voltage plateaus during discharging: 2.4, 2.2, and 2.0 V. The highest one corresponded to the breakage of the central S—S bond, the middle one originated from the formation of phenyl persulfide and phenyl sulfide radicals, and the lowest one was caused by the formation of Li_2S and lithium thiophenolate. The electron-withdrawing phenyl

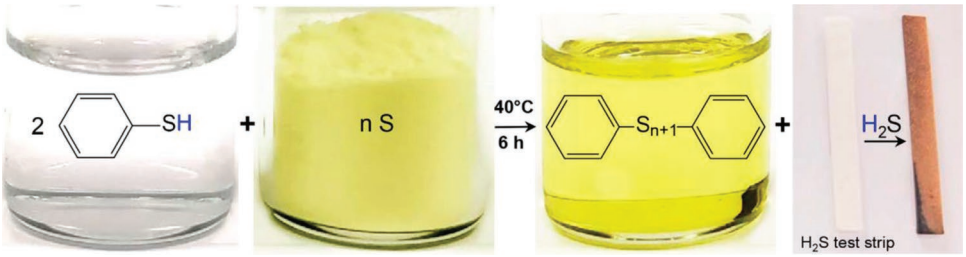

Figure 3. Visual representation of the synthesis process of phenyl polysulfide. Reproduced with permission.[30] Copyright 2018, American Chemical Society.

group raises the electrochemical potential of sulfur, which was beneficial for cathode materials. Finally, coin cells with phenyl polysulfides as cathode materials, and CNT papers as the host, were assembled and tested. PHS delivered the highest specific capacity of 650 mA h g^{-1} and a capacity retention of 80% in 500 cycles at 1 C (1 C = 774.5 mA g^{-1}).

Fu's group has studied the reaction mechanism of a variety of organosulfur compounds as cathode materials for LSBs.[31–33] In 2016, they used DMTS as a model to study the redox reactions in the cells. A four electron reaction pathway was discovered as shown in **Figure 4**a.[34] XRD and X-ray photoelectron spectra (XPS) results indicated that $LiSCH_3$ and Li_2S were the primary discharge products. Furthermore, gas chromatography-mass spectrometry test of the charged samples confirmed the existence of $LiSSCH_3$, dimethyl disulfide (DMDS), and dimethyl tetrasulfide (DMTtS). Based on these results, a possible reaction pathway was proposed as shown in Figure 4a. DMTS transformed into $CH_3S\cdot$ and $CH_3SS\cdot$ at first as the 3 e^- π bond stabilized the $CH_3SS\cdot$ radical. The radicals could react with Li^+ to form $LiSCH_3$ and $LiSSCH_3$ (reaction 5 and 6) or couple to form DMDS and DMTtS (reaction 3 and 4). The similar orbital potential energies of lowest unoccupied molecular orbital of Li^+ and highest occupied molecular orbital of the radicals and excessive Li^+ made reaction 5 and 6 the majority ones. Finally, the electrochemical performance of DMTS was tested with a multiwalled carbon nanotube (MWCNT) paper as the host. At an ultralow electrolyte/DMTS ratio of 3:1 mL g^{-1} and the high area loading of DMTS of 11.3 mg cm^{-2}, an initial specific discharge capacity of 7.42 mA h cm^{-2} at a current density of 0.1 C (1 C = 849 mA g^{-1}) could be achieved, 5.67 mA h cm^{-2} could be maintained after 30 cycles. In 2017, they further studied the reaction mechanism of dipentamethylene thiuram tetrasulfide (PMTT), one kind of thioether with N containing ring structures at both ends.[35] Like in DMTS, an asymmetrical cleavage of S—S bond occurred at first with $C_5H_{10}NC(S)S\cdot$ and $C_5H_{10}NC(S)SSS\cdot$ radicals formed. The $C_5H_{10}NC(S)SSS\cdot$ radical would take one Li^+ and break into $C_5H_{10}NC(S)S\cdot$ and $LiSS\cdot$, which would react with Li^+ to form $C_5H_{10}NC(S)SLi$ and Li_2S at the end. With excessive Li^+, planar delocalized π-orbitals would form as the electrons of N center flow to S, with one more Li^+ taken. The XPS results of PMTT cathodes collected at different stages of cycling confirmed the reaction pathway as shown in Figure 4b.

The low conductivity of S as well as organosulfur molecules hinders their application as electrode materials. Se has a much

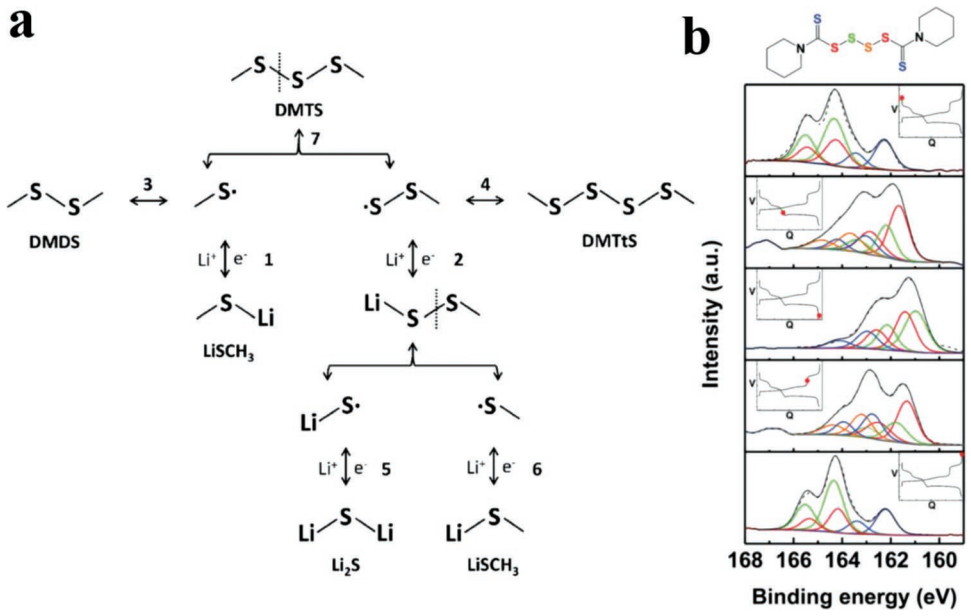

Figure 4. a) Proposed reaction pathway of DMTS. b) S 2p XPS spectrum of PMTT collected at different stages of charge and discharge. The color of the S labeled in the structure is a guide to the S deconvoluted in the spectrum. a) Reproduced with permission.[34] Copyright 2016, Wiley-VCH. b) Reproduced with permission.[35] Copyright 2017, Royal Society of Chemistry.

higher conductivity (10^{-5} S cm^{-1}) but lower specific capacity than S. Selenosulfide compounds could get a compromise of both conductivity and capacity. Cui et al.[36] studied phenyl selenosulfides as cathode materials for LSBs. Phenyl diselenide (PDSe) would transfer into PhSe· radical, which would attack the sulfur ring to form phenyl selenosulfides with different length of sulfur chain. With introducing S, the theoretical specific capacity of PDSe (171.7 mA h g^{-1}) increased to 311.4 and 427.4 mA h g^{-1} for PDSe–S and PDSe–S_2, respectively. The electrochemical properties of PDSe and PDSe–S/PDSe–S_2 were much different. PDSe only had one discharge/charge voltage platform; PDSe–S/PDSe–S_2 had three distinct discharge voltage platforms, corresponding to the reversible break and formation of Se—S and S—S bonds. Among all three samples, PDSe–S_2 had the highest initial specific capacity of 330 mA h g^{-1} at a current density of 0.2 C (1 C = 427.4 mA g^{-1}) and a good cyclic stability up to 200 cycles with a capacity retention higher than 73%. Besides, Guo et al.[37] studied the properties of phenyl selenosulfide with only one Se atom and one S atom. It turned out that phenyl selenosulfide had better electrochemical performance than those of phenyl disulfide and PDSe, which was ascribed to the higher entropy and lower Gibbs free energy that led to much less agglomeration in the discharged electrodes.

Above all, multistep reactions occurred when these organic molecules were utilized as electrode materials, except those with only two sulfur atoms. However, to understand the mechanism of multistep reactions, advanced characterization technology and computational simulations are needed. The properties of these molecules can be altered by designing the structure: sulfur atoms can bond with different organic groups including alkyl, vinyl, and aryl. The electrochemical potential, solubility, density, stability, as well as many other properties of these molecules can be tuned. It is also worth exploring host materials for small organic molecules, as these compounds may be in the liquid phase or soluble in the electrolyte. CNT papers or aerogels are the most widely used hosts. But the synthesis of CNT is complicated and CNT is easy to aggregate, which will reduce the available pore structure. Graphene aerogel, which is easier to synthesize, has also been reported as host of small organosulfur molecule for LSBs. Transition metal-based compounds can be introduced to further improve the absorption ability of the host. MXene, another type of 2D conductive material might also be suitable for sulfur host. The metal components in MXene, usually Ti and V, have stronger absorption ability toward organosulfur molecules than nonpolar carbon materials. Besides, the high catalyst activity of MXene will promote the dynamics, which is beneficial for high utilization of S and high rate performance.

4. High Sulfur Content Copolymers

High sulfur content copolymers can be easily synthesized through a copolymerization reaction between elemental sulfur and unsaturated monomers. The unique properties of sulfur make this copolymerization reaction possible. Sulfur tends to catenate and form a crown-shaped *cyclo*-S_8 under ambient conditions. When heated to over 159 °C, ring-opening polymerization occurs. S_8 turns into linear polysulfane with radical ends, which can react with unsaturated monomers to form high sulfur content copolymers. The lithiation and delithiation route of these copolymers are similar to S_8. Li_2S, together with R–S–Li (or R–Li), are the discharged product.

Pyun's group first reported the synthesis of poly(sulfur-random-1,3-diisopropenylbenzene) (poly(S-r-DIB)) through the copolymerization between sulfur and DIB at above 159 °C; no additional initiators or organic solvents are needed (**Figure 5**a).[38] They called it an inverse vulcanization process as a large amount of sulfur was used, which is inverse to conventional vulcanization process where a small amount of sulfur is used to stabilize the polydiene. The sulfur content in this compound can be tuned by adjusting the mass ratio of sulfur and monomers. A series of copolymers with sulfur content ranging from 50% to 90%, corresponding to 10–44 S units per DIB unit, were synthesized. The high sulfur content, which enables high energy density, is beneficial for the practical application of organosulfur compounds. The electrochemical behavior of these compounds was similar to S_8, two voltage plateaus at ≈2.3 and ≈2.1 V were detected. The copolymer delivered an initial specific capacity of 1100 mA h g^{-1} with a capacity retention of 823 mA h g^{-1} at 100 cycles at a current density of 0.1 C (1 C = 1672 mA g^{-1}). The mechanism of S-DIB was further studied by Pyun's group.[39] They systematically studied the electrochemical performance of S-DIB samples with different S contents. It was found that the specific capacity increased as the sulfur content increased at first, with those of 5%, 10%, and 15% by mass DIB exhibited high initial capacities and low capacity decay rate. Those with 20% or higher by mass DIB showed similar or worse performance compared with pure S. A possible reaction pathway was proposed. In the high voltage platform, higher order organosulfur DIB units and Li_2S_8 were formed, which were further reduced to lower order organosulfur DIB units and Li_2S_4. Then in the lower voltage platform, the lower order organosulfur DIB units and Li_2S_4 converted into fully discharged organosulfur DIB products and insoluble mixture of Li_2S_3 and Li_2S_2. It was also found that the organosulfur units in the discharged products functionalized as "plasticizer" to suppress irreversible deposition of the discharge products and enabled better cyclic stability.

Inspired by this work, poly(S-r-DIB) incorporated with CNT and graphene oxide (GO) were reported by others. Hu et al. reported a dual-confinement strategy to synthesize high-performance sulfur-copolymers for LSBs as shown in Figure 5b.[40] The CNT matrix was synthesized on an anodic aluminum oxide (AAO) template, then S-DIB copolymer was introduced through a melt-diffusion process. The sulfur content was 67%, lower than pure S-DIB copolymers in Pyun's work. But this compound showed higher initial specific capacity and long cycle stability: 1300 mA h g^{-1} at 0.1 C and 880 mA h g^{-1} at 1 C after 100 cycles with a capacity retention of over 98%. The better electrochemical performance was ascribed to the well-designed structure. CNTs framework and C—S covalent bond provided physical and chemical confinement of lithium polysulfides, respectively. Also, CNTs facilitated ion and electron transfer and accommodated the volume change of sulfur during charge and discharge. Shen et al. used an extrusion 3D printing strategy to fabricate 3D sulfur copolymer-graphene architecture (3DP-pSG) for the first time (Figure 5c).[41] S_8, DIB monomers, and

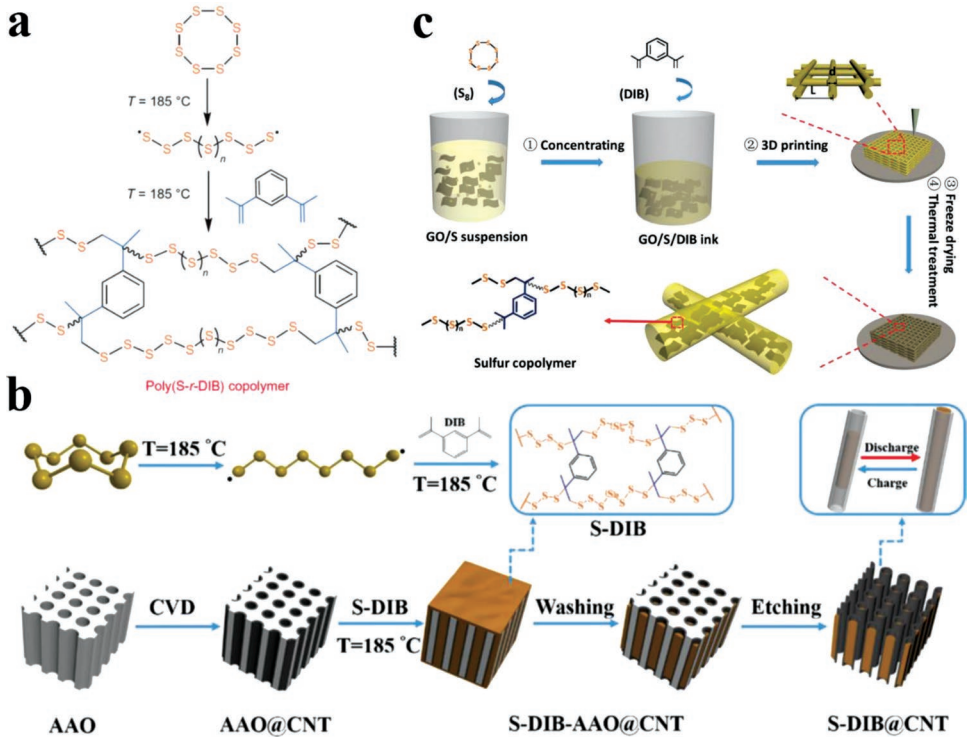

Figure 5. a) Synthetic scheme of poly(sulfur-random-1,3-diisopropenylbenzene) (poly(S-r-DIB)). b) Fabrication process of S-DIB@CNT. c) Schematic demonstration of 3D printing sulfur copolymer-graphene (3DP-pSG) architectures. a) Reproduced with permission.[38] Copyright 2013, Springer Nature. b) Reproduced with permission.[40] Copyright 2017, Wiley-VCH. c) Reproduced with permission.[41] Copyright 2018, Wiley-VCH.

graphene oxide were embedded in the 3D architecture. An in situ copolymerization process took place at 200 °C. Similarly, the GO framework provided high electrical conductivity and buffered the volume change. The sulfur content in 3DP-pSG reached 75.0%. This compound delivered a reversible capacity of 812.8 mA h g^{-1} at a current density of 50 mA g^{-1}. However, after 50 cycles, only 43% of the initial capacity was maintained.

Apart from DIB, there are other monomers that have been used to synthesize sulfur-copolymers. Li et al. reported a facial two-step process to synthesize high sulfur-containing copolymer (**Figure 6**a).[42] The S powder was heated to 180 °C under an Ar atmosphere, then triallyl isocyanurate (TAIC) was added into the molten S at a controlled mass ratio. The mixture was cooled to room temperature after reacting for several hours. Finally, the product was synthesized through heating the samples at 250 °C for 4 h under Ar atmosphere and referred to as S-triallyl isocyanurate organosulfur polymer composite (STI). It was found that STI had a "watermelon-seed" structure, the monoclinic S was the seed and the copolymer is the wrapper. This unique structure had several merits. First, a high sulfur content of 90% can be realized. Second, the superfine distribution of monoclinic S provides transport channels for ions and electrons. Finally, copolymer frameworks and C—S bonds suppress the generation and diffusion of lithium polysulfides. Consequently, STI had a high reversible capacity of 1123 mA h g^{-1} at 0.2 C (1 C = 1675 mA g^{-1}) and a good long term stability of 827 mA h g^{-1} after 200 cycles at 0.5 C with a decay rate of 0.043% per cycle.

Though high sulfur content copolymers can suppress the shuttle effect, the electrical conductivity of polymers is insufficient. Kang et al. studied how the structure of linkers affect the electrical conductivity and further affect the electrochemical performance of copolymers.[43] Four linker molecules based on quinone and triazine were investigated: tetra(allyloxy)-1,4-benzoquinone (TABQ), 2-allyloxy-naphthoquinone (ANQ), 1,4-bis(allyloxy)-anthraquinone (BAAQ), and triallyloxy-triazine (TATA). Density functional theory revealed that TABQ has the lowest bandgap in both single molecules and dimers linked by sulfur, which promises a high sulfur utilization and fast redox kinetics (Figure 6b). This also showed the possibility of tuning the properties of high sulfur content copolymers by designing the structure of monomers. As expected, among the four synthesized copolymers, Poly(S-TABQ) with a sulfur content of 75% had the best performance. The batteries based on poly(S-TABQ) had a high initial specific capacity of 1346 mA h g^{-1} at a current density of 0.1 C (1 C = 1670 mA g^{-1}). Exceptionally, a discharge capacity of 833 mA h g^{-1} could be achieved at a super high current density of 10 C. XPS tests of samples after 100 cycles showed that the change in intensity of C—S bond in poly(S-TABQ) is negligible, while in poly(S-TATA), a significant reduction of C—S content was determined. Also, poly(S-TABQ) showed lower Ohmic resistance and charge transport resistance.

Selenium sulfide or Se-doped S (Se_xS_y) has been used as a substitution of elemental S to synthesize sulfur-containing copolymers because of the high electrical conductivity of Se (≈10^{-3} S m^{-1}). In 2017, Zhou et al. reported an organosulfur cathode made from SeS_2. Se-doped poly (diallyl tetrasulfide) (PDATtSSe) was synthesized by using diallyl sulfide as a monomer and SeS_2 as the source of sulfur and selenium.[44] The content of S and Se in PDATtSSe was calculated to be

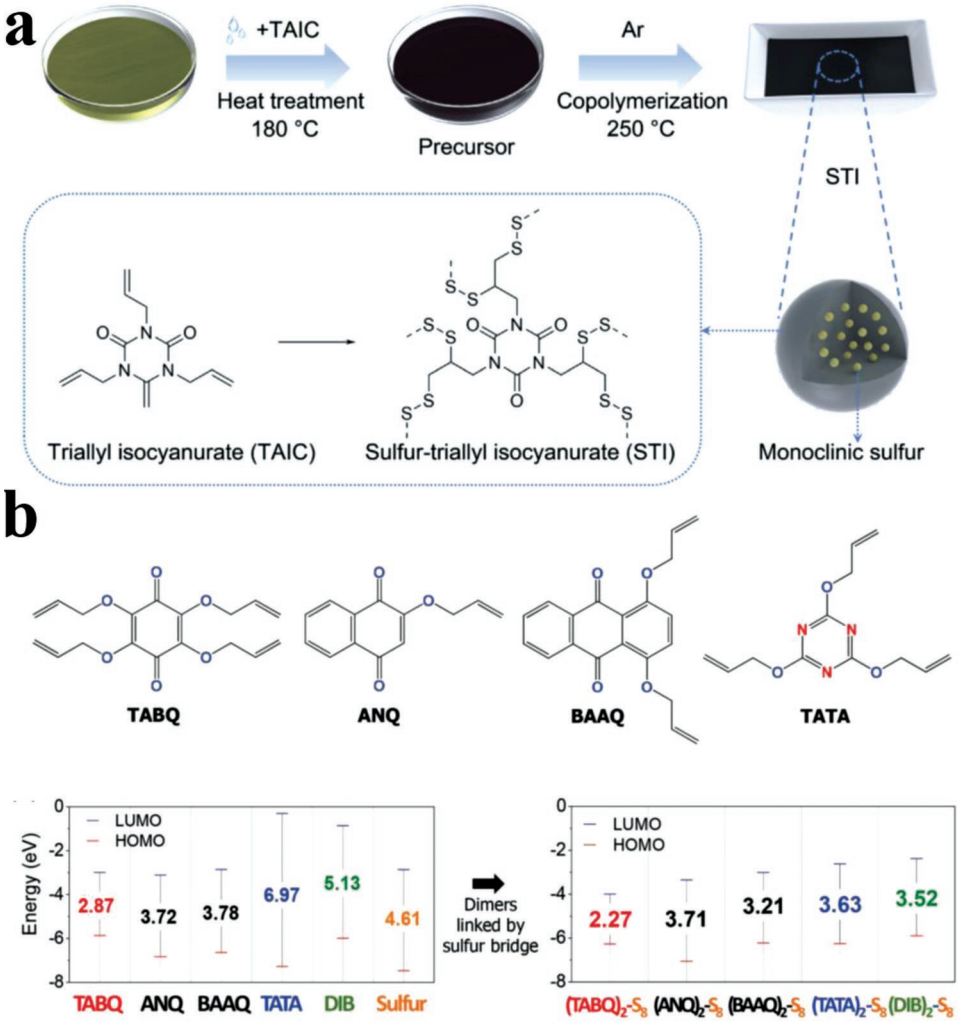

Figure 6. a) Schematic illustration of the synthesis process of STI and proposed chemical structure. b) Molecular structures of TABQ, ANQ, BAAQ, and TATA as well as the corresponding calculated energy diagrams of these compounds and their dimers with sulfur bridge. a) Reproduced with permission.[42] Copyright 2020, Elsevier. b) Reproduced with permission.[43] Copyright 2018, Wiley-VCH.

71.6%. When tested, PDATtSSe delivered a specific capacity of 700 mA h g^{-1} at a current density of 200 mA g^{-1} (based on the mass of PDATtSSe). A reversible capacity of 500 mA h g^{-1} and a low decay rate of 0.02% per cycle were achieved after 400 cycles at 600 mA g^{-1}. Then in situ UV/vis spectroscopy test revealed that no soluble lithium polysulfides formed during discharge and charge as no peak shifting was detected. SEM images also showed that a smooth and uniform solid-electrolyte-interphase (SEI) layer formed upon the lithium foil, indicating that the shuttle effect was greatly alleviated. Also, lower charge transfer resistance and faster Li^+ diffusion coefficient were found in samples with Se-doping. The effect of content of Se on the electrochemical performance of Se-doped high sulfur content copolymers was studied by Gomez et al.[45] A low energy and scalable process like that used in Pyun's work to synthesize S-DIB was applied to prepare poly(Sulfur-r-Selenium-r-DIB). The mixture of S and Se with different mole ratios was heated to 180 °C, DIB monomer was added once the mixture was melted. A different electrochemical behavior was observed with Se doping. In CV curves, two more peaks at 2.2 and 1.9 V were observed, which originated from the formation of polysulfoselenide and lower order lithium selenides. Among the copolymers with different Se contents, $Se_{0.05}S_{0.95}$-DIB and $Se_{0.075}S_{0.925}$-DIB had the best performance with initial specific capacities of 860 and 880 mA h g^{-1} at a current density of 0.2 C, and low capacity decay rates of 0.14% and 0.4% per cycle, respectively. Further increase in Se content would lead to the decrease of capacities as Se has a lower theoretical specific capacity than S.

Except for those synthesized from elemental S and monomers, high sulfur content copolymers could also be synthesized through the reaction between sulfides and monomers. In 2017, Preefer et al.[46] reported a high sulfur content material with only one point of S–S scission for LSBs, as shown in **Figure 7**a. This material has a high sulfur content (about 50% in atom number) and high theoretical specific capacity of 609 mA h g^{-1} based on six moles of Li per C_6S_6 monomer unit. Besides, the highly charged state of the discharge product, $C_6S_6^{6-}$, is insoluble in ether-based electrolyte, which eliminates the shuttle effect. The Raman spectra of samples at different state confirmed the reversible break and formation of S—S bonds, as the peak

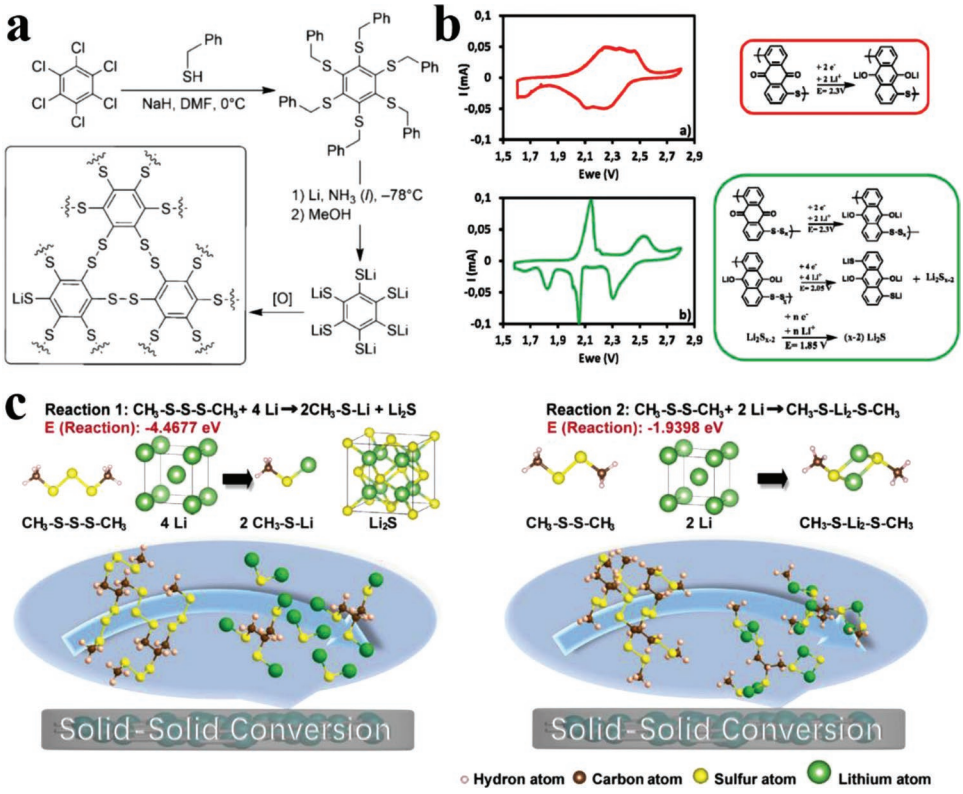

Figure 7. a) Synthesis scheme of cross-linked disulfide active materials. b) CV curves of PAQS (red) and PAQnS (green) at the second cycle and the proposed reaction pathway. c) Calculation of energy changes of possible lithiation reactions, bond length, and possible reaction formula for CH_3–S–S–S–CH_3 (Reaction 1) and CH_3–S–S–CH_3 (Reaction 2). Schematic diagrams of proposed electrochemical conversion are under corresponding reactions. Reproduced with permission.[46] Copyright 2017, Wiley-VCH. b) Reproduced with permission.[47] Copyright 2018, American Chemical Society. c) Reproduced with permission.[48] Copyright 2021, Elsevier.

at 480 cm^{-1} receded and enhanced repeatedly. A new peak at 270 cm^{-1} at the discharge state was assigned to −S−Li of the discharge product. Polyanthraquinones is one type of widely used organic electrode materials for batteries because of their high cyclic stability and abundance in nature. The low theoretical specific capacity of 225 mA h g^{-1} limited their application. Gomez et al.[47] synthesized a series of poly(anthraquinonyl sulfides) (PAQxS) with different lengths of S chain ($2 \le x \le 9$) through the reaction between 1,5-dichloroanthraquinone and sodium polysulfides in NMP solution at 120 °C. The introduction of S greatly changed the reaction pathway of PAQxS as shown in Figure 7b. For PAQS, a broad signal between 2 and 2.5 V was observed, which is unique for anthraquinones. For PAQnS (n means nine sulfur atoms per unit), three reduction peaks could be observed. The broad peak for anthraquinones shifted to 2.3 V and became sharp. The other two peaks at 2.0 and 1.7 V could be ascribed to the formation of polysulfides and Li_2S. Zhang et al.[48] proposed a strategy to eliminate shuttle effects in high sulfur content copolymers through controlling the length of the S chain and enabling a solid-solid reaction pathway. Trisulfide polymers and disulfide polymers were synthesized through the interfacial polymerization between sodium polysulfides and 1,2,3-trichloropropane. The length of S chain in the as-synthesized polymers could be controlled by adjusting the length of S chain in sodium polysulfide precursor. The in situ UV/vis and visual test of the electrolyte indicated that there was no shuttle effect and a solid–solid conversion took place as shown in Figure 7c.

In general, high sulfur content copolymers are easy to prepare and have relatively high capacities. Alkene and alkyne are the most commonly used monomers as they are the simplest and most frequently investigated organic compounds that have unsaturated groups. Another kind of widely used monomer is thiols. Because of the instability of S−H bond, thiols react easily with S at a relatively low temperature. Besides the physical and chemical properties of copolymers can be adjusted by designing the structure of monomers and controlling the ratio of S/monomers.[49,50] The electrical conductivity of copolymers is lower than expected. Introducing carbon materials to improve conductivity is a possible solution. Heteroatom doping might also be a strategy. The doping elements have higher conductivity or increase the density of electrons to lower electron transfer resistance. What's more, the reaction mechanism of these copolymers has not been fully understood. Models have been proposed to explain the electrochemical behaviors, but there are still debates about it. The reaction pathway is not clear. Some reported the breakage of terminal bonds at first and then the internal bonds, while others reported the opposite pathway. The breakage of C−S bonds on the ends of S chains is debatable, different final products such as R–Li and R–S–Li have been reported. Advanced characterization technology as well as simulation works are still needed to figure out the actual reactions of these copolymers.

5. Sulfurized Polymers

Polymers with unsaturated or reactive groups can also react with sulfur to form sulfurized polymers. However, the reaction condition is more rigid than those of monomers, usually involves high temperature, inert gas protection, and solid state milling. Meanwhile, during the high-temperature treatment, C—H bonds may break and gases (H_2S, SO_2, etc.) will be released. But the improved electrical conductivity and structural stability are also fascinating.

Among all sulfurized polymers that have been studied in LSBs, sulfurized polyacrylonitrile (SPAN) is the most popular one ever since the first report from Wang's group in 2002.[51] The good electrochemical properties and compatibility with carbonate electrolyte is attractive. The research about revealing the reaction mechanism and the structure of SPAN as well as designing and synthesizing SPAN-based materials with high performance are advancing. The formation of C—S covalent bond has been widely characterized and accepted. Recent research showed that there might be a S-containing ring structure. There is also research using carbon materials to improve the electrical conductivity or metal oxides to improve the stability of PAN. Other sulfurized polymers such as thiourea aldehyde resin (TAR)[52] and poly(acrylic acid) (PAA)[53,54] have also been investigated.

6. Sulfurized Polyacrylonitrile

Ever since Wang's report, SPAN has attracted more and more attention. The ability to suppress the shuttle effect, compatibility with carbonate electrolyte, and low self-discharge is intriguing. The research about SPAN is mainly about two aspects. First, the structure of SPAN and the reaction mechanism. Although a ladder structure in SPAN is commonly accepted, some details are divergent. The formation mechanism of C—S bond is unclear and the quantitative analysis is rare. For example, how many S atoms are bonded with C and the length of the S chain or ring have never been studied. What's more, some reports reported physically absorbed S in SPAN together with covalently bonded S. In the charge–discharge process, the C—S bond will break and form repetitively and this is not clear. Different final discharge products and reaction pathways have been reported. Besides a rational structure is needed to explain the high initial capacity and low Coulombic efficiency at the first cycle. Second, developing new synthesis method and incorporation of other components (carbon materials, metal oxides and heteroatom doping methods) to achieve a satisfactory performance are also needed.

7. Structure of Sulfurized Polyacrylonitrile

When Wang et al. first reported the synthesis of SPAN, they proposed a structure that elemental S_8 is embedded in the framework of pyrolytic PAN. However, in 2004, Yu et al. reported the existence of C—S bonds in SPAN.[55] Fourier transform infrared (FTIR), Raman spectra, and XPS confirmed the existence of C—S bonds. Specifically, for samples prepared at 450 °C, the structure with a backbone of N-containing ring structure and a side chain with two sulfur atoms was proposed. Later, Wang et al. reported a single electron discharge process of SPAN cathodes, and the higher specific capacity than theoretical specific capacity of S was ascribed to the intercalation between Li^+ and the local environment surrounding the nitrogen (**Figure 8**a).[56] Recently, Weret et al. comprehensively studied the synthesis mechanism, chemical structure, and lithiation/delithiation pathway of SPAN.[57] During the synthesis, at above 170 °C, the ring opening polymerization of S_8 formed diradicals, which attacked C atoms in C≡N, and initiated the formation of heterocyclic structures (Figure 8b). Furthermore, at a higher temperature, dehydrogenation took place. However, the morphology change and mass loss after CS_2 washing also indicated the existence of physically confined S_8 in SPAN. During charge and discharge processes, Raman, FTIR, and solid-state NMR tests all proved the reversible cleavage and formation of C—S and N—S bonds, and the electron donating effect of Li—C and Li—N bonds increased the electron density of conjugated structures leading to the decrease of charge/discharge voltage hysteresis after the second cycle.

Though many models have been proposed to explain the electrochemical properties of SPAN from different aspects, many of them are debatable.[58,59] In some reports, the bonds between the terminal S atoms and carbon atoms break and reform during the charge and discharge process while others not. And the formation of N-S bonds is only reported by some recent articles. It is also noteworthy that the synthesis condition including reaction time, temperature, and mass ratio of S/PAN will affect the structures and the electrochemical properties of SPAN. High temperature and long reaction time will lead to less physically absorbed S as S is easy to evaporate. And the chain length or size of the cycle may be affected by the mass ratio of the precursors.

8. Performance of Sulfurized Polyacrylonitrile

The conjugated structure of SPAN can increase the electrical conductivity to some extent, but it is still far from satisfactory. Attempts have been made to solve these problems. Nuli's group synthesized PAN@CNT and PAN@graphene nanosheets composite materials to improve the electrical conductivity of SPAN.[60,61] Through in situ polymerization, PAN formed a core–shell structure with CNT or were anchored on the surface of graphene nanosheets, which provided better chemical interaction than physical mixing. As a result, the electrodes with CNT or graphene nanosheets had higher capacities than the counterparts (**Figure 9**a,b), especially at high current densities. Chen et al. used selenium sulfur composite (Se_xS) to synthesize Se-doped sulfurized PAN (Se_xSPAN).[62] The higher electrical conductivity of Se enabled the fast diffusion of Li^+, thus providing fast reaction kinetics and suppressing the shuttle effect (Figure 9c). With a small amount of Se-doping, $Se_{0.06}$SPAN exhibited a high reversible capacity of 1300 mA h g^{-1} at a current density of 0.2 A g^{-1}. This compound is compatible in both ether- and carbonate-based electrolytes.

Besides the innovation of electrodes, there is research about developing electrolyte additives, binders, etc. for SPAN-based

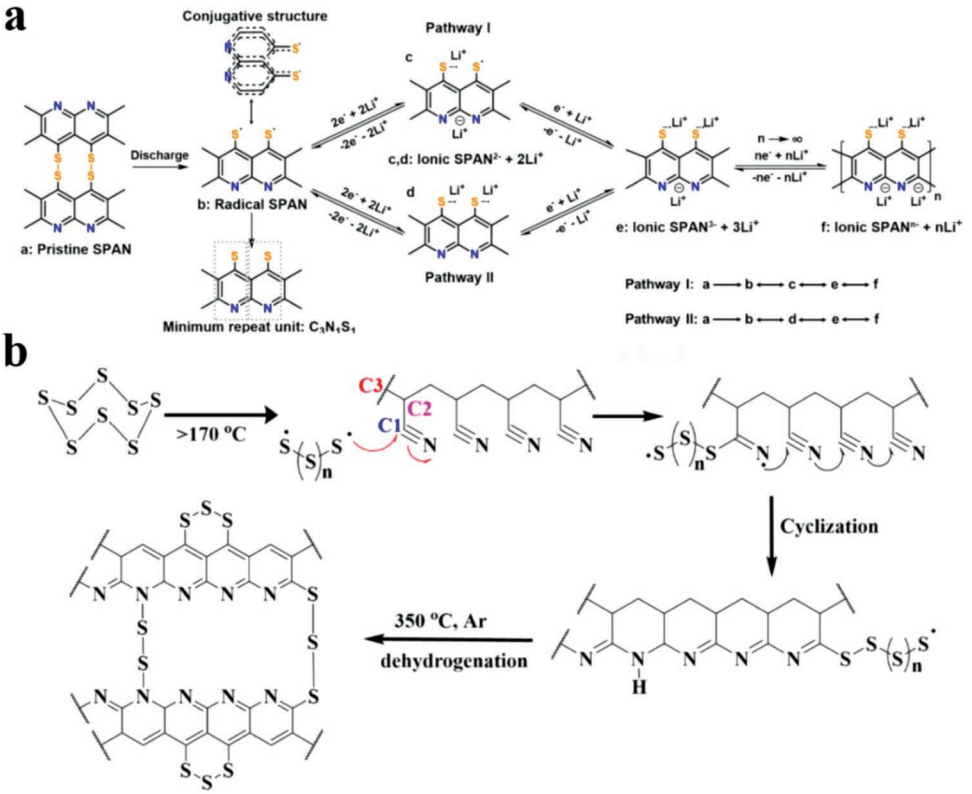

Figure 8. a) Possible reaction pathways of SPAN. b) Proposed reaction mechanism of synthesizing SPAN. a) Reproduced with permission.[56] Copyright 2018, American Chemical Society. b) Reproduced with permission.[57] Copyright 2020, Elsevier.

materials. Phosphorus-rich compounds have been used to develop flame-retardant electrolytes. Yang et al. used triethyl phosphate and 1,1,2,2-tetrafluoroethyl-2,2,3,3-tetrafluoropropyl as the additive in electrolytes to provide flame-retardant properties and good stability. Batteries with this electrolyte were capable of operating at 60 °C.[63] $LiNO_3$, which has been found to protect the Li metal anode through forming robust SEI, is widely used as an additive in ether-based electrolytes for LSBs. But the effect of $LiNO_3$ on the cathode especially SPAN-based materials has been rarely studied. Xing et al.[64] found that $LiNO_3$ especially at relatively high concentration (0.5 M) favored the formation of robust cathode-electrolyte-interphase (CEI), and discourages the dissolution of polysulfide. XPS test revealed that species like Li_2SO_x and Li_2S/Li_2S_2 were formed in CEI. A thick layer of ≈27 nm covering the cathode could be observed from the TEM image directly. And crystal phases of LiF and $LiNO_2$ were detected. This protective CEI layer reduced the dissolution of polysulfides and enabled better cyclic stability (up to 100 cycles) than carbonate-based electrolyte.

9. Other Sulfurized Polymers

Liu's group has reported a series of sulfurized PAA material for LSBs. In 2019, they reported a novel 2D organic polysulfane grafted on carbon chain as the cathode material.[65] The KCl template was used to provide an ultrathin morphology with defects to minimize Li^+ diffusion pathway. KI was used to promote the reduction of S_8 to di- or tri-sulfur radicals, which substitute the carbonyl group in PAA through a coupling reaction (**Figure 10**a). The sulfur content in the as-synthesized organic polysulfane nanosheets (OPNS) can be controlled by adjusting the reaction time for 1 to 24 h. OPNS-72 (72 means a weight ratio of 72% of sulfur) synthesized at 8 h had a reversible capacity of 889 mA h g^{-1} at a current density of 1 C (1 C = 1670 mA g^{-1}). High area loading (9.7 mg cm^{-2}) electrodes were tested in this work. A capacity of 594 mA h g^{-1} was maintained after 400 cycles at 1 C, with a decay rate of 0.065% per cycle. Afterward, they further reported a flexible nanosheet with polysulfane grafted on porous graphene (pGPS), which had an excellent electrochemical performance. A high capacity of 1045 mA h g^{-1} at 1 C (1 C = 1670 mA g^{-1}) and good capacity retention of 95.3% after 100 cycles at 5 C.

Chen's group reported several sulfurized polymers with novel structures. In 2019, a TAR with sulfur-rich side chains was synthesized through a two-step process.[52] At first, a condensation between thiourea and formaldehyde took place, then the mixture of polymer and sulfur was kept at 170 °C for 8 h, forming a highly cross-linked compound (S-TAR). This structure has several advantages: 1) the hyper branched framework formed mesopores and provided higher electrical conductivity; 2) the combination of physical and chemical confinement suppresses the shuttle effect; 3) mesoporous structure provides abundant diffusion channels for Li^+. Importantly, ultraviolet–visible (UV–vis) spectroscopy was used to quantitatively measure the content of covalently bonded sulfur in S-TAR. It turned out that 51.0 wt% of sulfur was bonded with TAR. S-TAR had a high specific capacity of 1285 mA h g^{-1} at a

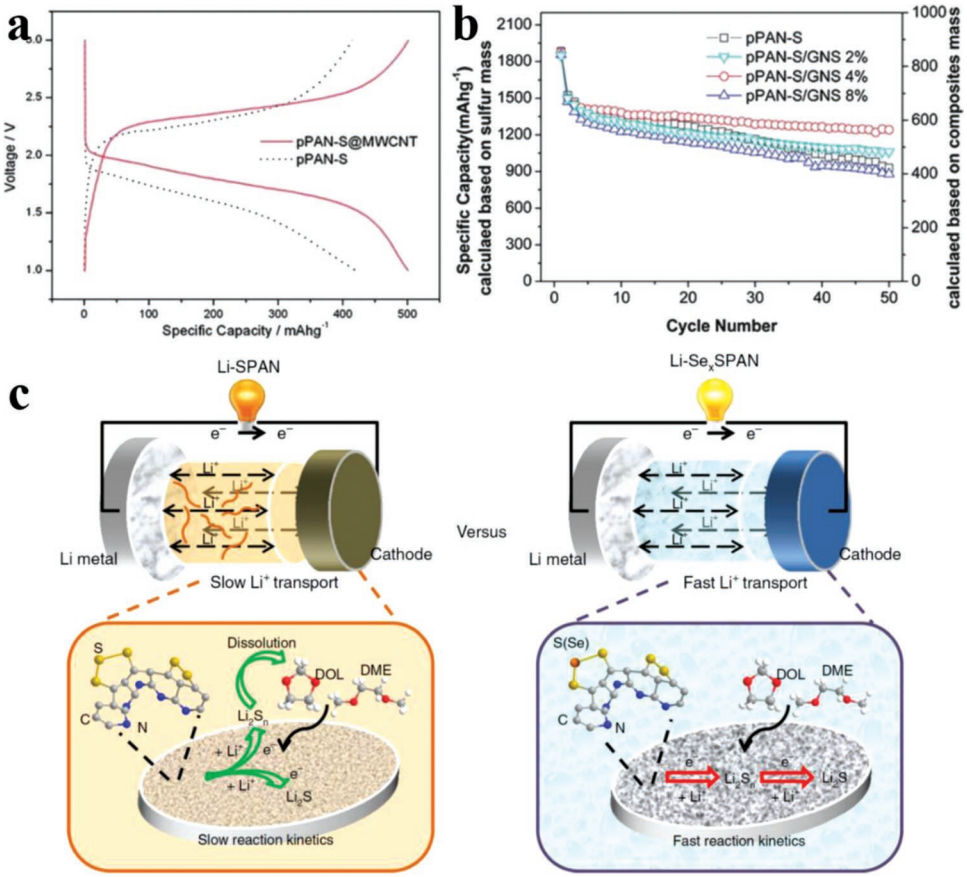

Figure 9. a) Charge–discharge curves of pure SPAN and SPAN@CNT tested as a current density of 1 C. b) Cyclic stability of SPAN and SPAN@GNS with different GNS content at a current density of 0.1 C. c) Schematic diagram of proposed reaction process of Se-doped SPAN. a) Reproduced with permission.[60] Copyright 2011, Royal Society of Chemistry. b) Reproduced with permission.[61] Copyright 2012, Royal Society of Chemistry. c) Reproduced with permission.[62] Copyright 2019, Springer Nature.

current density of 0.1 C (Figure 10b,c), and 819 mA h g^{-1} was maintained after 500 cycles at 1 C with a decay rate of 0.045% per cycle. Instead of using conductive components to improve electrical conductivity, using conductive polymers is also effective. Zeng et al. used poly(m-aminothiophenol) (PMAT), a conductive polymer with abundant thiol groups, to synthesize a highly cross-linked sulfurized polymer (S-PMAT).[66] Conductive PMAT enabled better conductivity and reactive thiol groups reacted with sulfur to form covalent bonds, suppressing the dissolution of lithium polysulfides. As a result, S-PMAT delivered a specific capacity of 1240 mA h g^{-1} at a current density of 0.1 C (1 C = 1670 mA g^{-1} as well as a high stability of 495 mA h g^{-1} at 2 C after 1000 cycles with a decay rate of 0.04% per cycle.

To impel the practical application of organosulfur compounds as cathodes for LSBs, the test under more practical condition, including pouch cell configuration, high area S loading, low electrolyte usage, and thinner Li foil is important. Recently, Yang et al.[67] reported a MOF-modified electrolyte system with suppressed solvent activity for SPAN-based cathode. An ultralow electrolyte usage of 1 µL mg^{-1} was applied to assemble pouch cells with a limited Li metal anode usage (0.4 time excessive). A specific capacity of 430 mA h g^{-1} could be achieved based on the total mass of both Li anode and S@pPAN cathode. He et al.[68] designed and synthesized a novel S@PAN/S_7Se composite as the cathode material. The sulfur particles were wrapped by Se-doped sulfurized poly acrylonitrile (PAN/S_7Se), which acted as an in situ block layer so that electrolyte could not penetrate. As a result, the SEI layer was formed mostly on the surface of PAN/S_7Se particles, which was more stable during the charge–discharge process. Pouch cells using this cathode delivered a specific capacity of 978 mA h g^{-1} at a current density of 0.1 A g^{-1}.

In summary, the electrochemical performances (including S content, specific capacity, and cyclic stability) as well as test conditions of different organosulfur compounds are listed in **Table 1**.

10. Organosulfur in Electrolytes for Lithium–Sulfur Batteries

The electrolyte plays an important role in LSBs. On one hand, the solid–liquid–solid reaction pathway enables fast reaction and high utilization of active materials. Soluble long-chain lithium polysulfides can be reduced to short-chain lithium polysulfides in the electrolyte, which is faster than solid-state reactions. And as the S on the surface of hosts is reduced to lithium polysulfides and dissolve in the electrolyte, the S inside

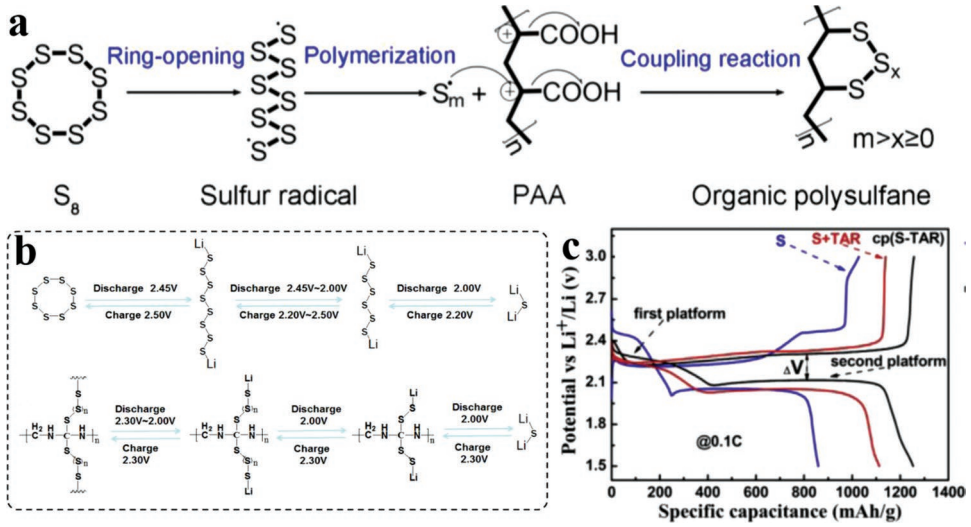

Figure 10. a) Proposed synthetic mechanism of organic polysulfane. b) Reaction pathways of S/C and cp(S-TAR)/C electrodes. c) Charge and discharge curves for LSBs with S/C, S+TAR/C, and cp (S-TAR)/C electrodes at a current density of 0.1 C. a) Reproduced with permission.[65] Copyright 2019, Elsevier. b,c) Reproduced with permission.[52] Copyright 2018, Elsevier.

is available for reaction, which is of high importance because of the insulating nature of S. On the other hand, the concentration gradient forces the soluble long-chain lithium polysulfides to diffuse between anodes and cathodes in the electrolyte. The long-chain lithium polysulfides can react with Li metal to form short-chain lithium polysulfides and Li_2S_2/Li_2S. The consumption and corrosion of Li anodes will lead to the formation of lithium dendrites and safety issues. The "dead" sulfur formed will lead to low efficiency and stability. To solve these problems, recently, organosulfur has been used as the electrolyte additive from two aspects: 1) provide new reaction pathways or improve the reaction kinetics and suppress shuttle effects;[76–78] 2) change the composition and properties of SEI for high stability.[79–82]

Xie et al. introduced sulfur container additives to the electrolyte to improve the performance through reversible storage and release of lithium polysulfides intermediates (**Figure 11** a).[77] Di(tri)sulfide polyethylene glycol (PES_n), the sulfur container, can store and release sulfur by reversibly lengthening and shortening sulfur chains. The high reactivity of sulfur container with sulfur could be verified by the fast reaction between PES_n and Li_2S_8/Li_2S, Li_2S_8 solution turned light orange immediately and white Li_2S suspension turned yellow. Also, the PES_n facilitated a unique and uniform deposition of Li_2S, the aggregation of Li_2S will lead to low efficiency in the charge process. Consequently, batteries with PES_n exhibited an enhancement in capacity and stability by 151 mA h g^{-1} after 100 cycles at 0.5 C (Figure 11b). However, these highly reactive compounds may lead to severe self-discharge behavior. Gupta et al. introduced an additive (methyl trifluoroacetate [CH_3TFA]) that could react with lithium polysulfides to form lithium trifluoroacetate (LiTFA) and dimethyl polysulfides, both of which enhanced the performance of LSBs.[76] The high donor number of LiTFA inhibited the clustering of the polysulfide intermediates, which lowers the amount of lithium polysulfides for further reactions, even under lean electrolyte condition. Meanwhile, the dimethyl polysulfides could alter or enhance the reaction pathways and showed high stability with lithium metal anodes. Pouch cells with CH_3TFA additive at high sulfur loading (4.8 mg cm^{-2}) under the lean electrolyte condition (4.5 µL mg^{-1}) had a capacity of around 700 mA h g^{-1} after 40 cycles. Chen et al.[82] proposed an in situ solidification strategy for efficient blocking of polysulfides by using a chloro-containing additive, 2,5-dichloro-1,4-benzoquinone (DCBQ) in the electrolyte. Once formed, polysulfides would be covalently fixed by DCBQ via nucleophilic substitution reactions along with the formation of a solid S-DCBQ organosulfur polymer. The reaction between polysulfides and DCBQ could be evidenced by the color difference of the Li_2S_6 containing electrolytes with and without DCBQ. Solid organosulfur particles could also be detected. XPS results confirmed the substitution of the chlorine atoms in DCBQ by sulfur atoms. Besides, the benzoquinonyl group could accelerate the lithium ion transport and promote the reactions. The batteries with DCBQ had higher initial specific capacity (about 1200 mA h g^{-1}, 400 mA h g^{-1} higher than those without DCBQ) and better cyclic stability with 92% capacity retention after 100 cycles at a current density of 1 C.

Constructing artificial SEI through the reaction between organosulfur additives in the electrolyte and lithium metal anodes is a promising way of stabilizing lithium metal anodes for LSBs practical application. Li et al. reported a flexible and tough SEI layer through adding poly(sulfur-random-triallylamine) (PST) into electrolytes as an additive (Figure 11c).[80] PST reacted with Li to form lithium organosulfides (RS_6Li_6), lithium organopolysulfides (RS_xLi_6), lithium polysulfides, and Li_2S/Li_2S_2; the organic compounds functioned as "plasticizers" to make the hybrid SEI layer more flexible and stable. It was also found that too many PST additives in the electrolyte could result in lower stability, probably caused by increased consumption of lithium and a thicker hybrid SEI layer showing higher resistance. Finally, batteries with 8% PST additive had a Coulombic efficiency as high as 99% for 400 cycles at a current density of 2 mA cm^{-2} with a capacity of 1 mA h cm^{-2}. Wei et al. reported an organosulfur containing SEI as a shield to prevent lithium polysulfides from reacting with lithium metal

Table 1. Electrochemical performance of organosulfur compounds.

Cathode	S content [%]	Specific capacity [mA h g^{-1}]	Cyclic stability [%]
DMTS[34]	76.2	720 (0.1 C, 1 C = 849 mA g^{-1})	82 (50 cycles, 0.1 C)
PMTT[35]	50	406 (0.2 C, 1 C = 418 mA g^{-1})	87 (100 cycles, 0.2 C)
PHS[30]	55.5	650 (0.5 C, 1 C = 775 mA g^{-1})	80 (500 cycles, 1 C)
DMTS/3DFNG[29]	63.4	822 (0.1 C, 1 C = 849 mA g^{-1})	53.8 (500 cycles, 1 C)
DIXPS[28]	64.6	628 (0.1 C, 1 C = 672 mA g^{-1})	74 (1000 cycles, 4 C)
Poly(S-r-DIB)[38]	70	1100 (0.1 C, 1 C = 1672 mA g^{-1})	74.8 (100 cycles, 0.1 C)
SDIB@CNT[40]	63.5	1300 (0.1 C, 1 C = 1675 mA g^{-1})	98 (100 cycles, 0.1 C)
PDATtSSe[69]	72.6	700 (200 mA g^{-1})	92 (400 cycles, 600 mA g^{-1})
3DP-pSG[41]	75	812.8 (50 mA g^{-1})	43.4 (50 cycles, 50 mA g^{-1})
Poly(S-TABQ)[43]	75	1346 (0.1 C, 1 C = 1670 mA g^{-1})	74 (500 cycles, 1 C)
STI[42]	90	1123 (0.2 C, not mentioned)	94 (350 cycles, 1 C)
BTTP[49]	≈72	901.7 (901.7 mA g^{-1})	68.4 (120 cycles, 901.7 mA g^{-1})
PDATtS[50]	-	700 (200 mA g^{-1})	85 (300 cycles, 600 mA g^{-1})
SPAN[51]	53.4	850 (0.2 mA cm^{-2})	75 (50 cycles, 0.2 mA cm^{-2})
CSM-450[55]	35.2	520 (not mentioned)	92 (240 cycles, not mentioned)
SPAN@MWCNT[60]	63	697 (0.1 C, not mentioned)	85 (50 cycles, 0.1 C)
SPAN@GNS[61]	47	≈1850 (0.1 C, 1 C = 1675 mA g^{-1})	80 (100 cycles, 0.1 C)
S/cPAN[70]	51	860 (100 mA g^{-1})	57 (100 cycles, 100 mA g^{-1})
CoS_2/SPAN/CNT[71]	43.2	1799 (0.2 C, not mentioned)	880 mA h g^{-1} (400 cycles, 1 C)
Te_xS_{1-x}@pPAN[53]	47.6	1504 (0.1 A g^{-1})	87.3 (200 cycles, 0.5 A g^{-1})
$Se_{0.06}$SPAN[62]	47.2	1300 (0.2 A g^{-1})	0.029/cycle (800 cycles, 0.4 A g^{-1})
BP-SPAN[72]	43	2036 (0.1 C, 1 C = 1675 mA g^{-1})	46.6 (200 cycles, 1 C)
SPAN[73]	53.6	829 (0.2 C, not mentioned)	≈70% (200 cycles, 1 C)
S-PPy[74]	≈40	1222 (0.1 mA cm^{-2})	47 (20 cycles, 0.1 mA cm^{-2})
S/T-PPy[75]	30	1157 (0.1 mA cm^{-2})	56 (80 cycles, 0.1 mA cm^{-2})
cp(S-PMAT)[66]	≈80	1240 (0.1 C, 1 C = 1672 mA g^{-1})	66.9 (1000 cycles, 2 C)
cp(S-TAR)[52]	39	1285 (0.1 C, 1 C = 1672 mA g^{-1})	0.045/cycle (500 cycles, 1 C)
OPNS[65]	72	891 (1 C, 1 C = 1670 mA g^{-1})	0.014/cycle (620 cycles, 1 C)
pGPS	71	1045 (0.5 C, 1 C = 1670 mA g^{-1})	95.3 (1000 cycles, 5 C)

anodes.[79] 3,5-bis(trifluoromethyl)thiophenol (BTB), which reacted with lithium to form an organosulfur-containing SEI layer, was used as an additive in the electrolyte. The visualized test showed that BTB would react with lithium foils, but the formed SEI layer protected the lithium foil from further reaction, as assessed by the color of the lithium polysulfides solution which stayed light yellow after 16 h. It was believed that the Ph–S^- component, which was formed by the reaction between sulfhydryl groups in BTB and lithium metals, repelled lithium polysulfides by electrostatic repulsion. With BTB as the additive, cells with a more practical operating condition (high loading of 4.5 mg cm^{-2}, low E/S ratio of 5.0 µL mg^{-1} and an ultrathin lithium foil [50 µm]) delivered an initial capacity of 950 mA h g^{-1} and remained 700 mA h g^{-1} after 82 cycles at a current density of 0.1 C. In 2021, Lian et al.[33] reported a bifunctional electrolyte additive-benzenedithiols (BDTs), which changed the reaction pathway and the composition of SEI layers simultaneously. It was found that among all the three isomers of BDT: 1,2-BDT, 1,3-BDT, and 1,4-BDT, 1,4-BDT had the best performance, which could be ascribed to the lower steric hindrance in 1,4-BDT. The H atoms in the thiol groups in 1,4-BDT would be substituted by Li at the first discharge process to form Li_2-1,4-BDT. During the following charge process, Li_2-1,4-BDT would be delithiated to form $PhS_2\cdot$ radical, which tended to form oligomers like $C_{12}H_8S_6$ and $C_{12}H_8S_8$. The oligomers would act as the starting material in the next discharge process and underwent the cleavage of S—S bonds like other organosulfur molecules. 1,4-BDT also protected the Li metal anode through forming a stable, uniform, and dense organic–inorganic hybrid SEI. Much lower overpotential and uniform surface of Li metal could be observed from the Li//Li symmetric cells with 1,4-BDT as an additive. XPS tests revealed that new compounds like organic sulfur (Li_2-1,4-BDT) were formed in the SEI layer. Consequently, pouch cells with 1,4-BDT as the additive delivered an initial specific capacity of 943 mA h g^{-1} at a current of 300 mA with high area S loading of 6.5 mg cm^{-2} and ultralow electrolyte usage of 3.5 µL mg^{-1}. It is also worth mentioning that 1,4-BDT contributed to part of capacity of the cells, about 100 mA h g^{-1}.

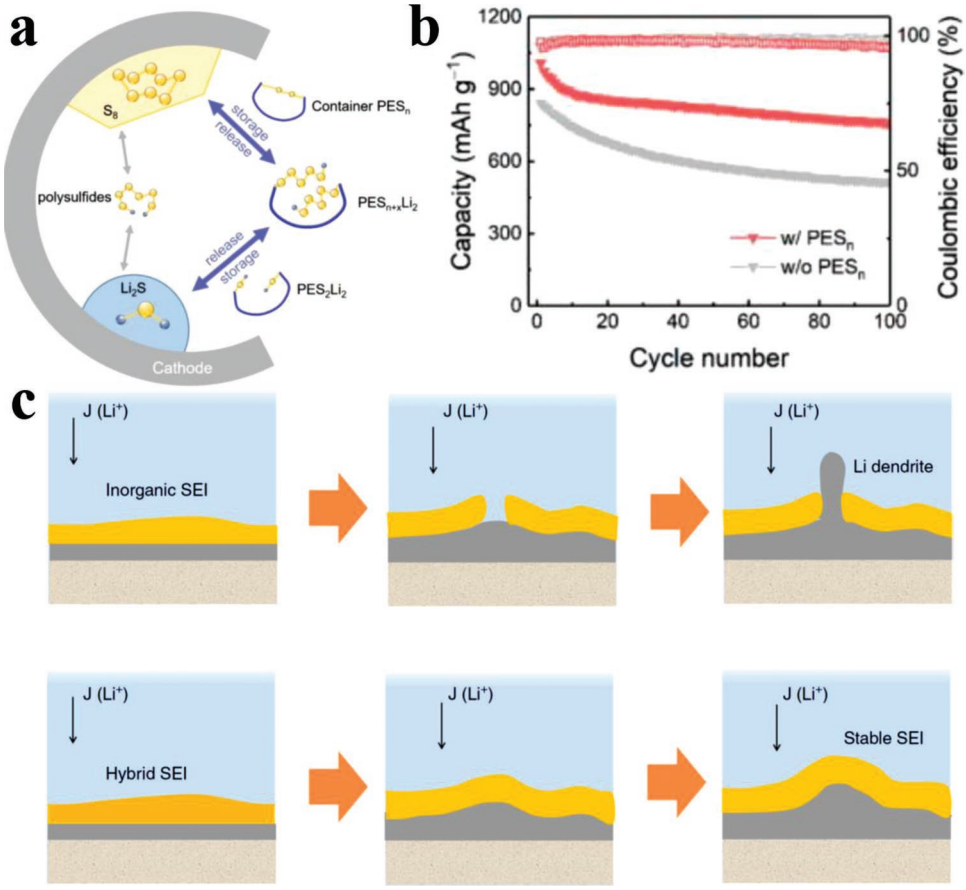

Figure 11. a) Working mechanism of sulfur container PES_n. b) Cyclic stability of LSBs with and without PES_n. c) Illustration of the protection of Li metal anodes by stable inorganic/organic hybrid SEI layers. a,b) Reproduced with permission.[77] Copyright 2019, Wiley-VCH. c) Reproduced with permission.[80] Copyright 2017, Springer Nature.

11. Organosulfur in Interlayers and Binders for Lithium–Sulfur Batteries

Functionalized interlayers and binders have also been applied to alleviate the shuttle effect in LSBs.[83–87] Adding an interlayer between cathode and separator with the ability to adsorb lithium polysulfides or accelerate the electrochemical reaction is an effective strategy to suppress shuttle effect and protect the lithium metal anodes. The interlayers should be thin, electrically conductive, and flexible, and most importantly should have components with the ability to adsorb the intermediates or accelerate the electrochemical reaction. Heteroatom-doped carbon materials, metal oxides/sulfides/phosphides, and metal–organic-frameworks have been studied as effective components in interlayers for LSBs. Wang et al. reported a SPAN-based functionalized interlayer for LSBs.[88] SPAN was synthesized by a similar process as other reports. After that, one side of separator was coated with a slurry made from SPAN, acetylene black, and carboxymethyl cellulose in a weight ratio of 8:1:1. It was found that this interlayer enabled higher utilization of sulfur and suppressed the shuttle effect. Batteries with this interlayer had a high initial capacity of 1338 mA h g^{-1}, and 65% capacity retention after 200 cycles at 1 C. However, it is also worth mentioning that SPAN itself contributed part of the total capacity of the batteries. This interlayer was not free-standing, instead it was coated on a Celgard separator.

Functionalized binders have been used to accommodate the volume change of electrode materials, and improve the electrical conductivity and stability of batteries. For example, cross-linked binders have been used for Si anodes to accommodate the volume change and improve the structural integrity.[89–91] In LSBs, Zeng et al. reported a comb-like ion-conductive organopolysulfide polymer binder to improve the electrodeposition of S and Li_2S.[92] The aggregation of insulating Li_2S and S_8 after discharge and charge processes will lead to high resistance of electrical/ionic conductivity and finally leads to poor long cycle stability. In this work, a polymer (PSPEG) was synthesized by the undiscriminated reaction between polyethylene glycol after grafting dichloro and Na_2S_x moieties. It was found that the $-S_x-$ bonds could act as mediator to improve the electrodeposition of Li_2S/S_8 and further suppress the aggregation and enhance the utilization of active materials and the cycling performance. The ether oxygen groups on the side chain could increase the Li^+ migration rate and improve the rate performance of LSBs. Batteries with only 1 wt% could deliver a capacity of 780 mA h g^{-1} after 100 cycles at a current density of 0.1 C (1 C = 1675 mA g^{-1}). However, when using this binder,

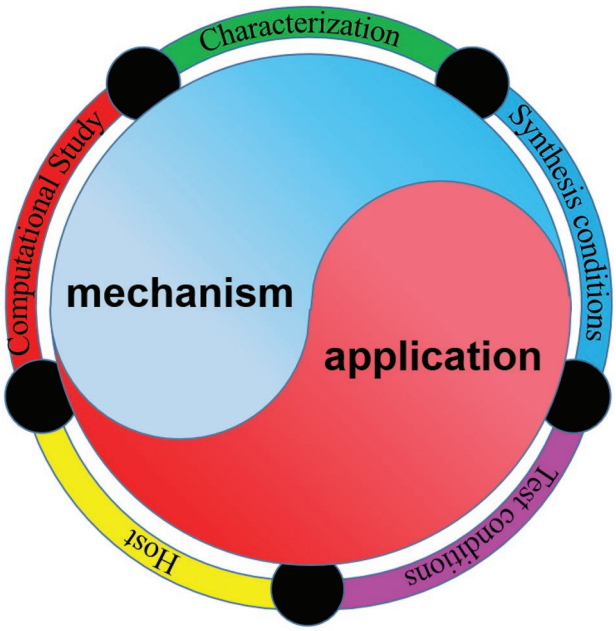

Figure 12. Illustration of suggestions for future research about organosulfur in LSBs.

the electrode material could easily peel off from aluminum foil current collectors and it was hard to cut into electrode disks for battery assembling.

12. Conclusions and Outlook

The progress of organosulfur in LSBs over the past years is discussed from three aspects: electrode materials, electrolytes, as well as interlayers and binders. Based on their structures and synthesis methods, organosulfur compounds are divided into three types. When used as cathode materials for LSBs, C—S covalent bonds are supposed to suppress or eliminate the shuttle effect. While the differences in their structures lead to different physical and electrochemical properties: color, density, voltage plateaus, specific capacity, stability, etc. For electrolytes, the application of organosulfur compounds has two merits: 1) accelerating the reactions through the intercalation between organosulfur additives and lithium polysulfides intermediates; 2) protecting the lithium metal anodes through forming functionalized SEI layers. The research about organosulfur for interlayers and binders in LSBs is rare, but it is worth further investigation. The application of interlayer and binder is facile. By using these components, sulfur hosts with complicated structures are not indispensable.

However, there are several issues to be addressed before the practical application of organosulfur in LSBs. First, the full understanding of the mechanism of electrochemical reactions in organosulfur electrodes. Though models have been proposed to explain their behaviors, none of them could explain all the behaviors. Second, as for electrode materials, the electrical conductivity of organosulfur is not satisfying and these compounds may be soluble in organic electrolytes. Third, the testing conditions, including areal sulfur mass loading, electrolyte/active material ratio, and current density, are not fully provided in most of the previous work. Finally, as for synthesized organosulfur compounds, the yield, which is essential for the practical application, is hardly mentioned.

Thus, we propose several suggestions for future research about application of organosulfur in LSBs (**Figure 12**). Advanced characterization technologies as well as computational stimulation will help understanding the mechanism. Technologies such as solid-state NMR, in situ Raman, in situ FTIR, XPS, and synchrotron-based soft X-ray absorption spectroscopy (XAS) can provide information about the structure and chemical state change of organosulfur compounds. For example, Shadike et al.[93] used XAS to study the reaction mechanism of 2,3,4,6,8,9,10,12-octathia biscyclopenta [b,c]-5,11-anthraquinone-1,7-dithione (TPQD), an organosulfur electrode material. The ex situ O K-edge XAS of samples at different state showed repeated disappearance and appearance of C=O bonds and C—O—Li bonds, indicating that C=O bonds contributed to the capacity of TPQD. In the S K-edge XAS, the peak originated from S=C bonds remained unchanged, indicating that S=C bonds were not involved in the reactions. The intensity of the peak of disulfide bonds (—C—S—S—C—) decreased upon lithiation, indicating that disulfide bonds broke and —C—S—Li formed. Meanwhile, a new peak of S–O σ^* in SO_3^{2-} or $COSO_2^-$ formed from the side reactions between —C—S—C— bonds and DOL electrolyte. Better understanding of the mechanism will also help researchers to design the structures of organosulfur compounds with improved performance. Machine-learning, which has been used in many research areas should be helpful in finding monomers and linkers with high performance. For examples, Sun et al.[94] conducted fast synthesis and machine-learning-assisted data diagnostics of 75 compositions for energy harvesting applications in 2 months. Also, a host or substrate with high electrical conductivity may improve the performance of organosulfur especially at high current densities. Besides, to push forward the commercialization of LSBs, the test conditions should be listed in detail. This will also help others to repeat the experiment and compare different materials. More practical test conditions should be applied to evaluate the performance of materials. The batteries with high-area sulfur loading, lean electrolyte usage as well as large-scale battery packs should be assembled and tested. The design of binders for high-area loading is necessary. Finally, as for synthesized materials, the synthesis condition and phenomenon as well as yield rate should also be clearly described. Some synthesis condition may be hazardous, toxic gases such as H_2S may be released, to which special attention needs to be paid. High yield rate is necessary for large scale application of organosulfur compounds.

Acknowledgements

Z.P. would like to thank the University College London and China Scholarship Council for a joint UCL-CSC PhD scholarship. The authors would like to thank Engineering and Physical Sciences Research Council (EPSRC, EP/V027433/1, EP/L015862/1, EP/R023581/1), the Royal Academy of Engineering under the Research Chairs and Senior Research Fellowships scheme (Brett), and the Royal Society (RGS\R1\211080; IEC\NSFC\201261) for funding support.

Conflict of Interest

The authors declare no conflict of interest.

Keywords

binders, cathodes, electrolytes, interlayers, lithium–sulfur batteries, organosulfur

Received: November 7, 2021
Revised: December 13, 2021
Published online:

[1] Q. Pang, X. Liang, C. Y. Kwok, L. F. Nazar, *Nat. Energy* **2016**, *1*, 16132.
[2] A. Manthiram, X. Yu, S. Wang, *Nat. Rev. Mater.* **2017**, *2*, 16103.
[3] A. Manthiram, Y. Fu, S. H. Chung, C. Zu, Y. S. Su, *Chem. Rev.* **2014**, *114*, 11751.
[4] C. Yang, X. Ji, X. Fan, T. Gao, L. Suo, F. Wang, W. Sun, J. Chen, L. Chen, F. Han, L. Miao, K. Xu, K. Gerasopoulos, C. Wang, *Adv. Mater.* **2017**, *29*, 1701972.
[5] N. W. Li, Y. Shi, Y. X. Yin, X. X. Zeng, J. Y. Li, C. J. Li, L. J. Wan, R. Wen, Y. G. Guo, *Angew. Chem., Int. Ed.* **2018**, *57*, 1505.
[6] H. Sun, G. Xin, T. Hu, M. Yu, D. Shao, X. Sun, J. Lian, *Nat. Commun.* **2014**, *5*, 4526.
[7] W. Liu, P. Oh, X. Liu, M. J. Lee, W. Cho, S. Chae, Y. Kim, J. Cho, *Angew. Chem., Int. Ed.* **2015**, *54*, 4440.
[8] J. Kim, H. Lee, H. Cha, M. Yoon, M. Park, J. Cho, *Adv. Energy Mater.* **2018**, *8*, 1702028.
[9] B. Xiao, H. Liu, J. Liu, Q. Sun, B. Wang, K. Kaliyappan, Y. Zhao, M. N. Banis, Y. Liu, R. Li, T. K. Sham, G. A. Botton, M. Cai, X. Sun, *Adv. Mater.* **2017**, *29*, 1703764.
[10] X. Ji, K. T. Lee, L. F. Nazar, *Nat. Mater.* **2009**, *8*, 500.
[11] T. Zhou, W. Lv, J. Li, G. Zhou, Y. Zhao, S. Fan, B. Liu, B. Li, F. Kang, Q.-H. Yang, *Energy Environ. Sci.* **2017**, *10*, 1694.
[12] D. Lei, K. Shi, H. Ye, Z. Wan, Y. Wang, L. Shen, B. Li, Q. H. Yang, F. Kang, Y. B. He, *Adv. Funct. Mater.* **2018**, *28*, 1707570.
[13] Y. Li, J. Fan, J. Zhang, J. Yang, R. Yuan, J. Chang, M. Zheng, Q. Dong, *ACS Nano* **2017**, *11*, 11417.
[14] S.-H. Yu, X. Huang, K. Schwarz, R. Huang, T. Arias, J. Brock, H. D. Abruna, *Energy Environ. Sci.* **2017**, 202.
[15] Y. Zhong, D. Chao, S. Deng, J. Zhan, R. Fang, Y. Xia, Y. Wang, X. Wang, X. Xia, J. Tu, *Adv. Funct. Mater.* **2018**, *28*, 1706391.
[16] J. Zhang, J. Y. Li, W. P. Wang, X. H. Zhang, X. H. Tan, W. G. Chu, Y. G. Guo, *Adv. Energy Mater.* **2018**, *8*, 1702839.
[17] J. He, L. Luo, Y. Chen, A. Manthiram, *Adv. Mater.* **2017**, *29*, 1702707.
[18] D. Xiao, Q. Li, H. Zhang, Y. Ma, C. Lu, C.-M. Chen, Y. Liu, S. Yuan, *J. Mater. Chem. A* **2017**, *5*, 24901.
[19] X. Liu, J.-Q. Huang, Q. Zhang, L. Mai, *Adv. Mater.* **2017**, *29*, 1601759.
[20] M. Li, H. Zhou, W. Yang, L. Chen, Z. Huang, N. Zhang, C. Fu, Y. Kuang, *J. Mater. Chem. A* **2017**, *5*, 1014.
[21] Y. Mi, W. Liu, X. Li, J. Zhuang, H. Zhou, H. Wang, *Nano Res.* **2017**, *10*, 3698.
[22] D. Liu, C. Zhang, G. Zhou, W. Lv, G. Ling, L. Zhi, Q. H. Yang, *Adv. Sci.* **2018**, *5*, 1700270.
[23] Z. Shadike, S. Tan, Q. C. Wang, R. Lin, E. Hu, D. Qu, X. Q. Yang, *Mater. Horiz.* **2021**, *8*, 471.
[24] H. Yang, J. Chen, J. Yang, J. Wang, *Angew. Chem., Int. Ed.* **2020**, *59*, 7306.
[25] X. Zhang, K. Chen, Z. Sun, G. Hu, R. Xiao, H. M. Cheng, F. Li, *Energy Environ. Sci.* **2020**, *13*, 1076.
[26] W. G. Lim, S. Kim, C. Jo, J. Lee, *Angew. Chem., Int. Ed.* **2019**, *58*, 18746.
[27] S. J. Visco, L. C. DeJonghe, *J. Electrochem. Soc.* **1988**, *135*, 2905.
[28] A. Bhargav, A. Manthiram, *Adv. Energy Mater.* **2020**, *10*, 2001658.
[29] J. He, A. Bhargav, A. Manthiram, *Energy Storage Mater.* **2019**, *23*, 88.
[30] A. Bhargav, M. E. Bell, J. Karty, Y. Cui, Y. Fu, *ACS Appl. Mater. Interfaces* **2018**, *10*, 21084.
[31] F. Li, Y. Si, Z. Li, W. Guo, Y. Fu, *J. Mater. Chem. A* **2020**, *8*, 87.
[32] F. Li, Y. Si, B. Liu, Z. Li, Y. Fu, *Adv. Funct. Mater.* **2019**, *29*, 1902223.
[33] J. Lian, W. Guo, Y. Fu, *J. Am. Chem. Soc.* **2021**, *143*, 11063.
[34] M. Wu, Y. Cui, A. Bhargav, Y. Losovyj, A. Siegel, M. Agarwal, Y. Ma, Y. Fu, *Angew. Chem., Int. Ed.* **2016**, *55*, 10027.
[35] A. Bhargav, Y. Ma, K. Shashikala, Y. Cui, Y. Losovyj, Y. Fu, *J. Mater. Chem. A* **2017**, *5*, 25005.
[36] Y. Cui, J. D. Ackerson, Y. Ma, A. Bhargav, J. A. Karty, W. Guo, L. Zhu, Y. Fu, *Adv. Funct. Mater.* **2018**, *28*, 1801791.
[37] W. Guo, A. Bhargav, J. D. Ackerson, Y. Cui, Y. Ma, Y. Fu, *Chem. Commun.* **2018**, *54*, 8873.
[38] W. J. Chung, J. J. Griebel, E. T. Kim, H. Yoon, A. G. Simmonds, H. J. Ji, P. T. Dirlam, R. S. Glass, J. J. Wie, N. A. Nguyen, B. W. Guralnick, J. Park, Á. Somogyi, P. Theato, M. E. Mackay, Y. E. Sung, K. Char, J. Pyun, *Nat. Chem.* **2013**, *5*, 518.
[39] A. G. Simmonds, J. J. Griebel, J. Park, K. R. Kim, W. J. Chung, V. P. Oleshko, J. Kim, E. T. Kim, R. S. Glass, C. L. Soles, Y. E. Sung, K. Char, J. Pyun, *ACS Macro Lett.* **2014**, *3*, 229.
[40] G. Hu, Z. Sun, C. Shi, R. Fang, J. Chen, P. Hou, C. Liu, H. M. Cheng, F. Li, *Adv. Mater.* **2017**, *29*, 1603835.
[41] K. Shen, H. Mei, B. Li, J. Ding, S. Yang, *Adv. Energy Mater.* **2018**, *8*, 1701527.
[42] X. Li, L. Yuan, D. Liu, Z. Li, J. Chen, K. Yuan, J. Xiang, Y. Huang, *Energy Storage Mater.* **2020**, *26*, 570.
[43] H. Kang, H. Kim, M. J. Park, *Adv. Energy Mater.* **2018**, *8*, 1802423.
[44] J. Zhou, T. Qian, N. Xu, M. Wang, X. Ni, X. Liu, X. Shen, C. Yan, *Adv. Mater.* **2017**, *29*, 1701294.
[45] I. Gomez, D. Mantione, O. Leonet, J. A. Blazquez, D. Mecerreyes, *ChemElectroChem* **2018**, *5*, 260.
[46] M. B. Preefer, B. Oschmann, C. J. Hawker, R. Seshadri, F. Wudl, *Angew. Chem., Int. Ed.* **2017**, *56*, 15118.
[47] I. Gomez, O. Leonet, J. A. Blazquez, H. J. Grande, D. Mecerreyes, *ACS Macro Lett.* **2018**, *7*, 419.
[48] X. Zhang, G. Hu, K. Chen, L. Shen, R. Xiao, P. Tang, C. Yan, H.-M. Cheng, Z. Sun, F. Li, *Energy Storage Mater.* **2021**, https://doi.org/10.1016/j.ensm.2021.11.014.
[49] P. Sang, J. Song, W. Guo, Y. Fu, *Chem. Eng. J.* **2021**, *415*, 129043.
[50] J. Zhou, X. Zhou, Y. Sun, X. Shen, T. Qian, C. Yan, *J. Energy Chem.* **2021**, *56*, 238.
[51] J. Wang, J. Yang, J. Xie, x. naixin, *Adv. Mater.* **2002**, *50*, 963.
[52] S. Zeng, L. Li, J. Yu, N. Wang, S. Chen, *Electrochim. Acta* **2018**, *263*, 53.
[53] S. Li, Z. Han, W. Hu, L. Peng, J. Yang, L. Wang, Y. Zhang, B. Shan, J. Xie, *Nano Energy* **2019**, *60*, 153.
[54] H. Hu, Y. Hu, H. Cheng, S. Dai, K. Song, M. Liu, *J. Power Sources* **2021**, *491*, 229617.
[55] X.-g. Yu, J.-y. Xie, J. Yang, H.-j. Huang, K. Wang, Z.-s. Wen, *J. Electroanal. Chem.* **2004**, *573*, 121.
[56] W. Wang, Z. Cao, G. A. Elia, Y. Wu, W. Wahyudi, E. Abou-Hamad, A. H. Emwas, L. Cavallo, L. J. Li, J. Ming, *ACS Energy Lett.* **2018**, *3*, 2899.
[57] M. A. Weret, C. F. J. Kuo, T. S. Zeleke, T. T. Beyene, M. C. Tsai, C. J. Huang, G. B. Berhe, W. N. Su, B. J. Hwang, *Energy Storage Mater.* **2020**, *26*, 483.
[58] X. Zhao, C. Wang, Z. Li, X. Hu, A. A. Razzaq, Z. Deng, *J. Mater. Chem. A* **2021**, *9*, 19282.
[59] B. He, Z. Rao, Z. Cheng, D. Liu, D. He, J. Chen, Z. Miao, L. Yuan, Z. Li, Y. Huang, *Adv. Energy Mater.* **2021**, *11*, 2003690.
[60] L. Yin, J. Wang, J. Yang, Y. Nuli, *J. Mater. Chem.* **2011**, *21*, 6807.
[61] L. Yin, J. Wang, F. Lin, J. Yang, Y. Nuli, *Energy Environ. Sci.* **2012**, *5*, 6966.

[62] X. Chen, L. Peng, L. Wang, J. Yang, Z. Hao, J. Xiang, K. Yuan, Y. Huang, B. Shan, L. Yuan, J. Xie, *Nat. Commun.* **2019**, *10*, 1021.
[63] H. Yang, C. Guo, J. Chen, A. Naveed, J. Yang, Y. Nuli, J. Wang, *Angew. Chem., Int. Ed.* **2019**, *58*, 791.
[64] X. Xing, Y. Li, X. Wang, V. Petrova, H. Liu, P. Liu, *Energy Storage Mater.* **2019**, *21*, 474.
[65] H. Hu, B. Zhao, H. Cheng, S. Dai, N. Kane, Y. Yu, M. Liu, *Nano Energy* **2019**, *57*, 635.
[66] S. Zeng, L. Li, L. Xie, D. Zhao, N. Wang, S. Chen, *ChemSusChem* **2017**, *10*, 3378.
[67] H. Yang, Y. Qiao, Z. Chang, P. He, H. Zhou, *Angew. Chem., Int. Ed.* **2021**, *60*, 17726.
[68] B. He, Z. Rao, Z. Cheng, D. Liu, D. He, J. Chen, Z. Miao, L. Yuan, Z. Li, Y. Huang, *Adv. Energy Mater.* **2021**, *11*, 2003690.
[69] J. Zhou, T. Qian, N. Xu, M. Wang, X. Ni, X. Liu, X. Shen, C. Yan, *Adv. Mater.* **2017**, *29*, 1701294.
[70] Y. Z. Zhang, S. Liu, G. C. Li, G. R. Li, X. P. Gao, *J. Mater. Chem. A* **2014**, *2*, 4652.
[71] A. A. Razzaq, X. Yuan, Y. Chen, J. Hu, Q. Mu, Y. Ma, X. Zhao, L. Miao, J. H. Ahn, Y. Peng, Z. Deng, *J. Mater. Chem. A* **2020**, *8*, 1298.
[72] S. Ma, Y. Wang, C. Fu, Y. Ma, Y. Gao, G. Yin, P. Zuo, *Chem. Commun.* **2020**, *56*, 12797.
[73] J. Lei, J. Chen, A. Naveed, H. Zhang, J. Yang, Y. Nuli, J. Wang, *ACS Appl. Energy Mater.* **2021**, *4*, 5706.
[74] M. Sun, S. Zhang, T. Jiang, L. Zhang, J. Yu, *Electrochem. Commun.* **2008**, *10*, 1819.
[75] X. Liang, Y. Liu, Z. Wen, L. Huang, X. Wang, H. Zhang, *J. Power Sources* **2011**, *196*, 6951.
[76] A. Gupta, A. Bhargav, A. Manthiram, *ACS Energy Lett.* **2021**, *6*, 224.
[77] J. Xie, Y. W. Song, B. Q. Li, H. J. Peng, J. Q. Huang, Q. Zhang, *Angew. Chem., Int. Ed.* **2020**, *59*, 22150.
[78] S. Gu, J. Jin, S. Zhuo, R. Qian, Z. Wen, *ChemElectroChem* **2018**, *5*, 1717.
[79] J. Y. Wei, X. Q. Zhang, L. P. Hou, P. Shi, B. Q. Li, Y. Xiao, C. Yan, H. Yuan, J. Q. Huang, *Adv. Mater.* **2020**, *32*, 2003012.
[80] G. Li, Y. Gao, X. He, Q. Huang, S. Chen, S. H. Kim, D. Wang, *Nat. Commun.* **2017**, *8*, 850.
[81] S. Bonakala, A. D. Pathak, A. Deyko, C. Christova, I. Rudra, G. Verbist, *ACS Appl. Mater. Interfaces* **2020**, *12*, 18101.
[82] K. Chen, R. Fang, Z. Lian, X. Zhang, P. Tang, B. Li, K. He, D.-w. Wang, H.-M. Cheng, Z. Sun, F. Li, *Energy Storage Mater.* **2021**, *37*, 224.
[83] J. Xie, H. J. Peng, J. Q. Huang, W. T. Xu, X. Chen, Q. Zhang, *Angew. Chem., Int. Ed.* **2017**, *56*, 16223.
[84] C. Li, Z. Xi, D. Guo, X. Chen, L. Yin, *Small* **2018**, *14*, 1701986.
[85] Y. He, Z. Chang, S. Wu, H. Zhou, *J. Mater. Chem. A* **2018**, *6*, 6155.
[86] J. K. Huang, M. Li, Y. Wan, S. Dey, M. Ostwal, D. Zhang, C. W. Yang, C. J. Su, U. S. Jeng, J. Ming, A. Amassian, Z. Lai, Y. Han, S. Li, L. J. Li, *ACS Nano* **2018**, *12*, 836.
[87] E. Cha, M. D. Patel, J. Park, J. Hwang, V. Prasad, K. Cho, W. Choi, *Nat. Nanotechnol.* **2018**, *13*, 337.
[88] F. Wang, X. He, *Mater. Lett.* **2019**, *256*, 126604.
[89] Q. Xu, J. K. Sun, Z. L. Yu, Y. X. Yin, S. Xin, S. H. Yu, Y. G. Guo, *Adv. Mater.* **2018**, *30*, 1707430.
[90] M. Chen, B. Li, X. Liu, L. Zhou, L. Yao, J. Zai, X. Qian, X. Yu, *J. Mater. Chem. A* **2018**, *6*, 3022.
[91] N. Kim, H. Park, N. Yoon, J. K. Lee, *ACS Nano* **2018**, *12*, 3853.
[92] F. L. Zeng, N. Li, Y. Q. Shen, X. Y. Zhou, Z. Q. Jin, N. Y. Yuan, J. N. Ding, A. B. Wang, W. K. Wang, Y. S. Yang, *Energy Storage Mater.* **2019**, *18*, 190.
[93] Z. Shadike, H. S. Lee, C. Tian, K. Sun, L. Song, E. Hu, I. Waluyo, A. Hunt, S. Ghose, Y. Hu, J. Zhou, J. Wang, P. Northrup, S. M. Bak, X. Q. Yang, *Adv. Energy Mater.* **2019**, *9*, 1900705.
[94] S. Sun, N. T. P. Hartono, Z. D. Ren, F. Oviedo, A. M. Buscemi, M. Layurova, D. X. Chen, T. Ogunfunmi, J. Thapa, S. Ramasamy, C. Settens, B. L. DeCost, A. G. Kusne, Z. Liu, S. I. P. Tian, I. M. Peters, J. P. Correa-Baena, T. Buonassisi, *Joule* **2019**, *3*, 1437.

Zhiyong Pan is currently a Ph.D. candidate in the Department of Chemistry at University College London. He obtained his B.E. (2014) in Material Chemistry from Nankai University and his M.S. (2017) in Chemistry and Physics of Polymers from Fudan University. His interests are in high-energy-density lithium–sulfur batteries, lithium-ion batteries, and carbon nanomaterials.

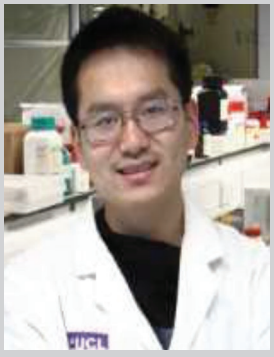

Guanjie He is an associate professor in materials chemistry at the University of Lincoln and an honorary lecturer at University College London (UCL). Dr. He received Ph.D. Degree in Chemistry, UCL under the supervision of Prof. Ivan P. Parkin. Dr. He's research focuses on materials design for electrochemical energy storage and conversion applications.

Ivan P. Parkin is a professor of materials chemistry, dean of Faculty of Maths and Physical Sciences at University College London. He is a selected fellow of Royal Society of Chemistry and a member of Academia Europaea. Prof. Parkin's work focuses on the development of functional materials and thin films for energy storage application, photocatalysis, and wetting.